POLITECNICO DI TORINO

Automotive Engineering
Master Degree

Master degree Thesis

Modelling and simulation of a shim valve for shock absorbers applications

Relatori
prof. Massimo Rundo

. . . .

Candidato
Manlio Terrana

. . . .

Academic year 2020-2021

Alla mia famiglia

Summary

This work wants to provide a method for the performance evaluation of a shim valve using the concept of discharge coefficient. The device used to test the procedure is a double tube damper, equipped with one shim valve, positioned between the compression chamber and reservoir. That valve is in charge of managing the excessive volume flow rate during the compression phase, it has direct implication on the device force vs speed characteristics. The investigated procedure follows three steps, where the valve or its components are tested through computer aided simulations. First objective is the computation of the shim stack deformation associated to the oil pressure. This is ensured by the use of the finite element analysis. The results of the first step are then used as input for the following analysis, where the relation between oil pressure and volume flow rate is obtained through the use of the computational fluid dynamics. At this point it is possible to compute the discharge coefficient by reversing the flow equation relative to orifices crossed by a volume flow rate under a certain pressure drop. This computation is limited by the variation of the system condition. Therefore third step of the procedure uses lumped parameter model, where the effect of the discharge coefficient is considered together with the flow area variation, to model as best as possible the damper behavior due to the shim valve effect. The particular geometry of the valve and the relative low computational power available, requires to simplify the geometry for the CFD analysis, not compromising the result accuracy. Three strategies for the valve simulation have been compared, showing pros and cons of each one. The results have been compared to data available for the model of damper tested. However the validation of this work requires the experimental test on the real damper, that can be considered as future development of this work.

Acknowledgements

I start by thanking professor Rundo, who tutored me, first in the activities and later in the drafting of this text, together with his collaborators Paola and Alessandro, who welcomed me to the fluid power research laboratory, making me feel at home. My greatest gratitude goes to my parents, who gave me the opportunity to follow the path towards the realization of my dreams, supporting me at all times and leaving me free to make my own choices. Together with my parents I want to thank my sister Teresa and my brother Carlo, who helped make me the person I am today. She was an example with her skills and her apprehension towards the whole family, he instead in his simplicity made me appreciate what life has in store for us, showing me that even the greatest difficulties can be overcome when accompanied by the right people. I want to thank my girlfriend Miriam, who was the best travel companion I could have, both figuratively and not, together we passed many exam sessions supporting each other, which we later celebrated around Europe. I hope that the trips together will not end even if the exams are over. I also want to thank her family, in particular Mimma and Giuseppe, who welcomed me and made me feel immediately at ease and who pamper me in their own way. Thanks go to my brother-in-law Francesco together with his family, who for me has always been a guide with his polite manners and his pragmatism. I thank my grandparents, both those in heaven and on earth, for having enriched my childhood and for having passed on to me those values that made the difference during my university career. A special thanks goes to my friends-roommates, Totò, Luigi, Gero and Salvatore. Who sweetened the hardest moments with their sympathy, that never made me feel alone away from home. In the same way I thank Stefano, David and Pedro together with the rest of the colleagues of the MEAU of Leiria, who during my Erasmus experience have been close to me, giving me support, rides at home and unbridled fun. Another big thank you goes to my automotive engineering colleagues, Daniel, Raffaele, Andrea, Luca, Nicolò, Gianluca, Matteo and Federico. With whom I not only collaborated in university projects but I also built a friendship relationship. I also want to thank the Turin Polytechnic and the City of Turin for making these six years unforgettable. Last but not least, I thank my friends from the south, Edison, Samuele, Ciccio, Arca, Roberta, Riccardo, Totò DP, Ferraro, with whom I enjoyed my life in the free moments from studying.

Contents

List of Tables

List of Figures

Part I

Generalities

Chapter 1

Nomenclature and symbols

Before to start the analysis on the shock absorber, it is good to present and explain the common vocabulary used in the power fluid field that is adopted in this text. Some abbreviations are used to streamline the text. In addition, dealing with mechanical systems, words are not enough to properly describe it, this text refers to the norm ISO 1219 that is universally used in power fluid. The units of measurement adopted are the ones of the SI but in some cases is widely accepted to use operatives units of measurements .

1.1 Abbreviations

The complete damper has been modeled from the hydraulic point of view thanks to the elementary blocks commonly used in power fluid related literature,that are representing the behaviour of the interaction between fluid and solid components. Blocks currently used are junctions, restictors, valves and so on. Abbreviations used in the text are summarized in table1.1.

Table 1.1: Abbreviations: List of abbreviations used in the text.

Symbol	Meaning
G	Junction
SF	Fixed restrictor
SV	Variable restictor
NR	Non return valve
Se	Reservoir
VC	Compression valve
VR	Rebound valve

1.2 Geometrical quantities

In order to perform the quantitative analysis of the system, during its working, the geometrical parameters that condition the damper behavior, need to be identified unequivocally. The surface on which oil pressure acts and the passage area for the oil flow are identified by different symbols to avoid confusion. The operative units of measurement together with the geometrical variables used to describe the system are presented in table 1.2

Table 1.2: Geometrical quantities: List of geometrical quantities used in the text.

Symbol	Meaning	measurement unit SI	measurement unit conventional
A	Surface of action	m^2	mm^2
S	Passage area	m^2	mm^2
V	Volume	m^3	dm^3 or l
D, d	Diameter	m	mm

1.3 Physical quantities

Geometrical quantities are not enough to describe the system, physical quantities need to be added to the description. Their symbol and unit of measurement are summarized in table1.3.

Table 1.3: Physical quantities: List of Physical quantities used in the text.

Symbol	Meaning	measurement unit SI	measurement unit conventional
x	Stroke	m	mm
f	Spring deformation	m	mm
k	Spring stiffness	N/m	N/m
F	Force	N	N, daN
v	Linear velocity	m/s	m/s
u	Fluid speed	m/s	m/s
Q	Volume flow rate	m^3/s	l/min
p	Pressure	Pa	bar

1.4 Functional definitions

From the operative point of view, the following characteristics are defined[1]:

- Compression : inward rod displacement.
- Rebound : outward rod displacement.

- Braking : damper reaction force due to the relative speed between attaching points.

1.5 Graphical symbols

Modeling the system from the hydraulic point of view can help in the comprehension of the general working. Each physical component is represented by a symbol referring to the ISO 1219 norm, the symbols are then connected mirroring the physical assembly functioning. Here the symbols are presented.

Table 1.4: ISO 1219 recall: List of elementary blocks used to model the damper.

Component	Symbol	Function
continuous line		working, return and supply line for hydraulic power transfer;
dotted line		pilot control line, it is used to actuate hydraulic components;
dashed thin line		drain or bleed line;
pipeline junction		connection between more than 2 pipes;
reservoir		store oil at ambient pressure
linear actuator	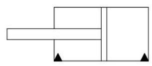	double acting differential cylinder with single piston rod;
fixed restrictor	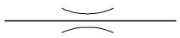	fixed orifice with viscosity dependent flow
variable restrictor	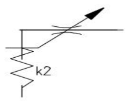	flow area is controlled by spring with fixed preload;
pressure relief valve	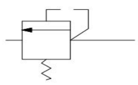	at the cracking pressure it throttles oil to keep the upstream pressure at the setting level;
non return valve		spring loaded check valve;

Chapter 2

Fluid mechanics principles

Damper technology is based on hydraulic principles. Looking the system with a simplified view, the first phenomenon that catches eye is the interaction between the double acting piston and the oil inside the chambers. The other crucial action is made by the oil throttled inside dedicated valves. To know the physics behind the system functioning is required in order to understand this text objective.Therefore the main hydraulic principles are presented in the following sections.

2.1 Pascal principle

In 17^{th} century Blaise Pascal has understood and then has divulged the nature of fluids inside closed chamber, that are transmitting the punctual pressure level variation to every point of the fluid, acting normally to the internal chamber surfaces.This principle is daily used by humankind, and is at the base for the developed analysis. Regarding to the working condition, the piston pushes the oil toward the chamber with positive volume variation and exchanges a force with it through the surface of action. That force is the son of the oil pressure that is due to the flow resistance.Therefore the damper braking force depends not only on the oil characteristics but also on the system geometry. Pascal principle holds in steady state conditions and normal operating condition are generally far from steady state. However the system will be analyzed in some different conditions, with the hypothesis of steady state flow condition, therefore the pressure inside each chamber is assumed constant during the phase of oil throttling.

2.2 Oil compressibility

One of the main difference between liquid and gas state is the compressibiliy. Fluids in gas form try to occupy all the available space in the container, liquids instead occupy only the required volume. Under compression action the gas volume varies strongly, instead liquids under compression shows a limited volume variation, that is appreciable at really high pressure with respect to normal operating conditions for hydraulic damping systems. The bulk modulus β is the parameter used to characterize the volume variation for liquid under compression, it is measured with the same unit of the pressure, and is expressed by the opposite of the ratio between pressure increment and relative volume variation, as shown in the following equation.

$$\beta = -\frac{dp}{\frac{dV}{V}}$$

For oil used in power fluids field the bulk modulus is around 1.5 GPa. In the application analyzed the maximum pressure value is far from the level at which volume variation is significant, therefore future computation will be under the assumption of non compressible liquid. Figure 2.1 illustrates the 2 phases for the estimation of the bulk modulus.

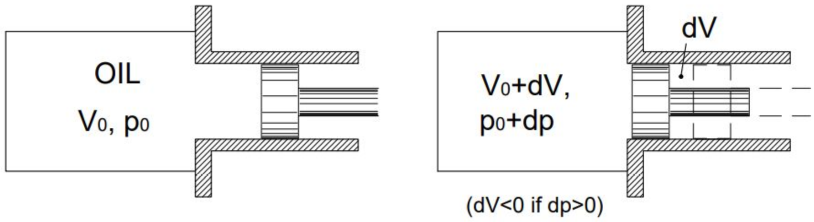

Figure 2.1: Bulk modulus estimation procedure.

2.3 Hydraulic resistances

In non ideal world friction exists, some time its presence can give advantages, for example walking will be impossible without friction, and in some cases it can be an issue, for example locking to the power waste in machines. Also fluids are affected by friction, that leads to power losses. Depending on the operating conditions, a differentiation can be made, hydraulic losses are distributed or local. Distributed losses due to internal fluid friction are present in long straight pipes and are proportional to the ratio pipe length over diameter. Local losses are concentrated in pipe bends or in that zones where a sudden restriction of the flow area is present. They are mainly related to the minimum flow area and the kind of flow. If the flow is in laminar regime, volume flow rate and pressure drop are simply proportional. In the case of turbulent regime, the volume flow rate is proportional to the square root of the pressure drop. Applying the Bernoulli's equation to two section of a pipe with a section restriction in between where the flow regime is turbulent, the following relation comes out:

$$Q = C_d S \sqrt{\frac{2\Delta p}{\rho}}$$

Where C_d is the discharge coefficient, that depends on the orifice shape and can be estimated with mathematical formulas for simple geometries[4]. Δp is the pressure

drop across the restriction. S is the flow area and ρ is the fluid density.
The power waste due to the restriction can be easily computed by the product of volume flow rate and pressure drop.

$$P_W = Q\Delta p$$

2.4 Restrictor behaviour

The restictor is a local resistance, where the important reduction of flow area can have 2 different effects. If a pressure drop is imposed across the restrictor it determines the volume flow rate and it is called metering behaviour. Instead when certain volume flow rate is enforced on a restrictor it determines a pressure drop and it is called compensator. The possibility to have a double effect make its function crucial in both the situation of controlling the force rather than the speed of an actuator. When the objective is the actuator speed, the correct volume flow rate needs to be set. Instead when the the goal is to exchange a certain force withe actuator, the pressure of the power source is the key. Figure 2.2 summarizes the causes and its effects for an hydraulic orifice.

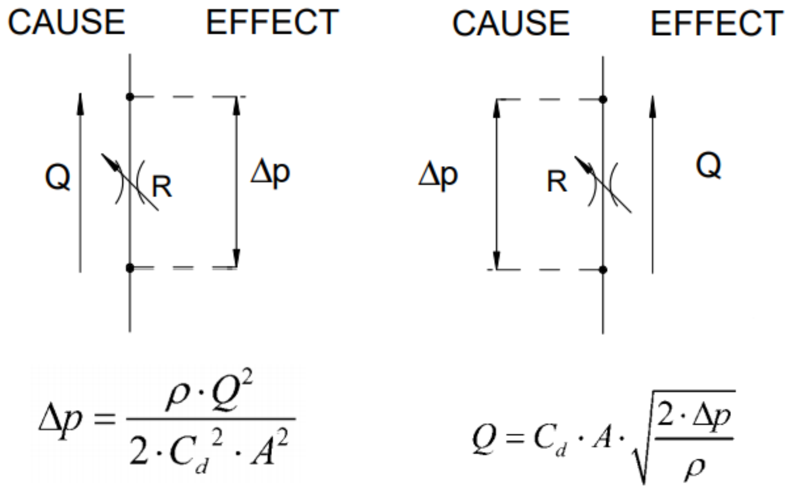

Figure 2.2: Restrictor behaviour illustration and associated equations.

Chapter 3

Hydraulic damper

Earth moving vehicles are provided by suspensions mostly for two reasons[3]:

- If the vehicle interacts with the road through more than three wheels, the system is hyperstatic, suspensions accomplish for the load distributions ensuring tire-rod contact , that can be affected by the road unevenness.

- To smooth the vibrations due to road asperities transmitted to the passengers.

Suspensions are so important that both bicycles and motorcycles use suspensions to ensure comfort and dynamic performance. Suspension systems are characterized by an elastic member and a dissipative one, called damper, the joining of the two is generally called shock absorber.In the years several technologies were proposed, driven by different objectives as kinetic energy regeneration rather then dynamic performance, but the most used one for massive production goods remains the classic hydraulic damper.

3.1 General working principle

An hydraulic damper is made by a double effect linear actuator and at least two valve groups, one with the task of controlling the oil flow between the two chambers and another one used to compensate the difference in volume between the two chambers, due to the presence of the rod only in one side of the piston. First valve mentioned is called rebound valve, instead the second one mentioned is called compression valve. The two valves use the deformation of a spring against the action of the oil pressure in order to regulate the flow. The spring that controls the flow can have several shapes, on the market it is possible to find dampers equipped with helical springs or more commonly, thin disks similar to a belleville spring called shims. Playing with the thickness and the number of disks, several braking characteristics could be obtained. The damper dissipates the kinetic energy forcing the oil to pass through an orifice, the volume flow rate is proportional to the piston speed that is assumed equal to the relative speed between the 2 attaching points of the damper. When a volume flow rate is imposed to pass through an orifice it is subjected to a pressure drop, this phenomenon allows to dissipate energy with a determined power. The pressure drop is affected by the orifice geometry. The equivalent spring stiffness influences the flow area directly. If that spring is soft, it will deform more allowing an higher oil flow, avoiding a fast increase of the pressure inside the oil chamber in opposition to the piston displacement, resulting in a small damper braking. Vice versa, if that spring has high stiffness, it will obstruct the oil flow and boost the pressure in the interested chamber, resulting in higher damper braking force. The correct working of the damper therefore is strongly dependent on the equivalent stiffness of the spring controlling the valves.

3.2 Typologies

Volume variation is not equal in magnitude for the two damper chambers, therefore during the working of the system some oil needs to be stored when it passes from the chamber with bigger active surface A to the one with smaller active surface a , vice versa when the flow is in opposite direction, some oil needs to flow inside the bigger chamber with less possible resistance to reduce cavitation phenomenon. Dampers are realized in two versions generally, double tube or single tube, figure 3.1 shows a section schematics for comparing the two kind of dampers. In the typology with two pipes, they are respectively fixed concentrically, the internal pipe is the guide for the piston that divides the two chambers. The volume between the two tubes is used as a reservoir for the oil volume compensation. In the single tube version instead the oil volume compensation is realized by a third chamber filled with gas, obtained within the main tube or by an external accumulator. For the first solution the accumulator is obtained in the bottom part of the pipe by using a floating piston, where the gas expands or is compressed regarding to the working phase. The other solution allows to reduce the overall dimensions and it is quite utilized in challenging applications.

3.3 Components

The mechanical system under investigation is realized with the assembly of several components, each one with its function. They must ensure not only the structural resistance but also the functional performance. Now the list of components together with their functions follows.

- Top ring: it is made in metallic material, it has inside a vulcanized rubber bushing to cut-off high frequency vibrations. The ring connects the damper to the vehicle body and it is welded to the top cap.

- Top cap: it is a metallic disk positioned between the top ring and the piston rod. It has the task of sustaining the dust shield, that generally is assembled by welding or threaded fastening.

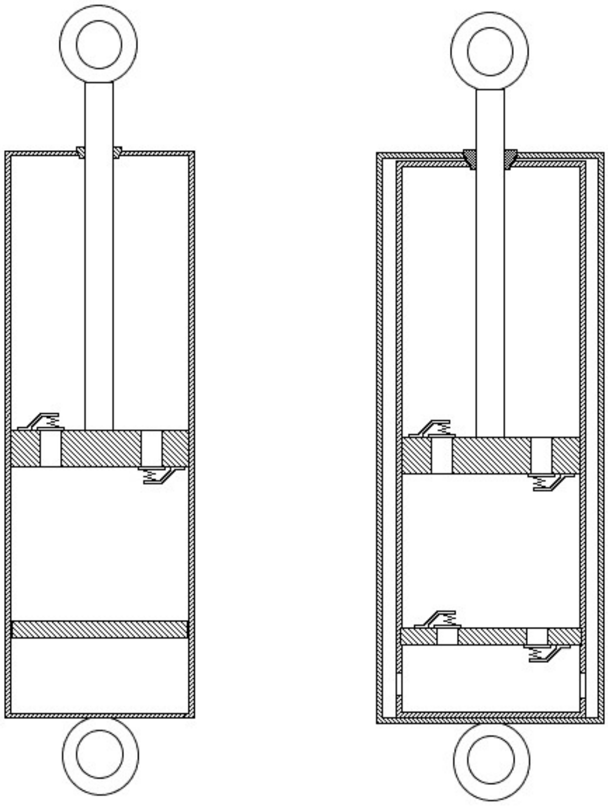

Figure 3.1: Damper typology: single tube in the right, double tube in the left.

- Dust shield: it is a cylinder made in metallic or polymeric material, it has no structural task but it is used to protect the rod from external agents as water, dust, mud, small stones that could scratch its sliding surface implying a fast sealing deterioration with consequences on oil leakages or contamination.

- Reservoir tube: it is the external metallic pipe and it has the function of collecting possible oil leakages from the top sealing and to be the reservoir for accomplish oil storing, in compression phase, and oil supply in rebound phase.

- Cylinder tube: it is the sleve for the piston containing most of oil used by the damper. Cylinder pipe is fixed concentrically to the reservoir tube. It is important to avoid the oil contamination by external agents both during assembly and working phase.

- rod guide: metallic fixed bushing, it closes both the reservoir pipe and the cylinder on the top side, giving the allocation for the sealing assembly. In case of oil leakages from the chamber on the rod side, it sends the oil from the sealing zone to the reservoir through an hole avoiding oil wasting.

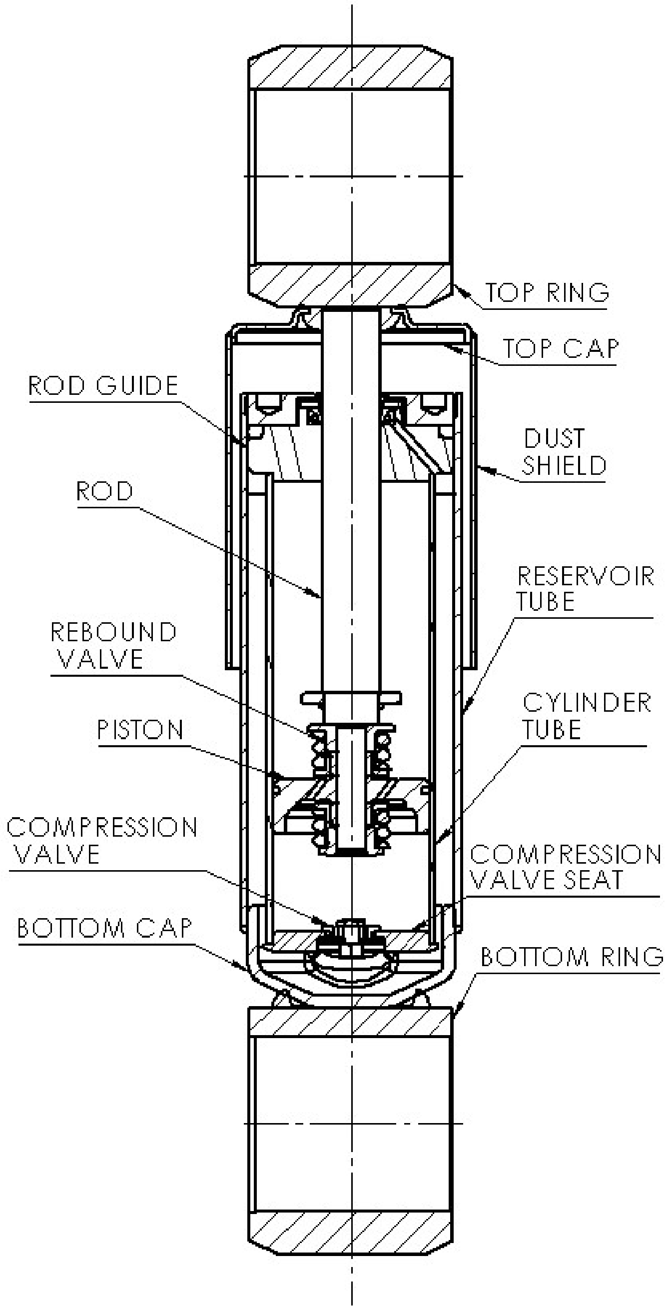

Figure 3.2: Damper model section view.

- Compression valve seat: it is a metallic disk fixed with interference in the bottom damper part, between the cylinder and the reservoir pipe. It has the function of closing the bottom chamber and within it is obtained the allocation for the compression valve.

- Bottom cap: it is a tapered metallic connection between the bottom damper part and the bottom ring. It has also some lands that bears the compression valve seat. It is generally welded to the bottom ring.
- Bottom ring: it has the same function of the top ring. Its shape can be different with respect to the top one for assembly reasons.
- Compression valve: this assembly has the function of throttling excessive oil volume flow rate during compression phase, and to ensure oil back flow when in rebound phase. The valve is constituted by a set of elastic elements that, when are deformed under oil pressure, allows a certain flow rate. The back flow is obtained through the complete valve body displacement that in this case assumes the function of a check valve.
- Rod: metallic cylindrical beam, used to connect the top ring with the piston, by its length depends the damper stroke, it also requires an optimum surface finishing in order to avoid fast sealing wearing. The rod diameter needs to be designed considering the maximum force to transmit and the effect on the displaced oil volume.
- Piston: cylindrical metallic component fastened to the rod by threaded junction. It is provided by cross holes with the function of metering restrictors. The piston itself is part of the rebound valve assembly.
- rebound valve: it is an assembly made by poppets and springs, mounted across the piston, that controls the oil flow between the two chambers.

3.4 Hydraulic model

The damper can be modeled from the hydraulic point of view by using the blocks presented in the section 1.5. They refers to the norm ISO 1219. The complete schematic is shown in figure 3.3, where the cylinder and the piston are modelled by using a differential double effect linear actuator, the chamber at the top is the one provided by smaller active surface a due to the rod presence, its value is computed starting from the diameters magnitude and it has an annular shape.

$$a = \frac{\pi(D^2 - d^2)}{4}$$

The other active surface has a circular shape, therefore its magnitude is easily computed by using the relation for the Area of the circle. The others functional components are the two valves groups. The VC is modelled with two restrictors in series that are in parallel to a NR valve. First restrictor S3 is fixed and represent the group of holes that are connecting the chamber 2 to the second restrictor SV2, that instead has a variable flow area,that is sensible to the upstream pressure, it represent the shims coupling with their retainer. Then on the top left of figure 3.3 the VR is modelled, it is constituted by two circuit branches in parallel, one is modeled with two restrictors, SV1 that has a variable flow area sensible to the pressure at the junction G2 and S1 that has fixed geometry and represents the cross holes on the piston that are connecting the two chambers. In the other branch the situation is similar to the previous one but flipped in the succession order. In this case to model the pressure sensible part of the assembly it is used a simple valve, normally closed by a spring with fixed preload and by the pilot pressure signal coming from the chamber 1. Possible leakages from the rod guide are taken into account by adding the drain on the chamber 1,toward the reservoir. The explanation about the two fundamental valves for the damper will go deeper in the following sections.

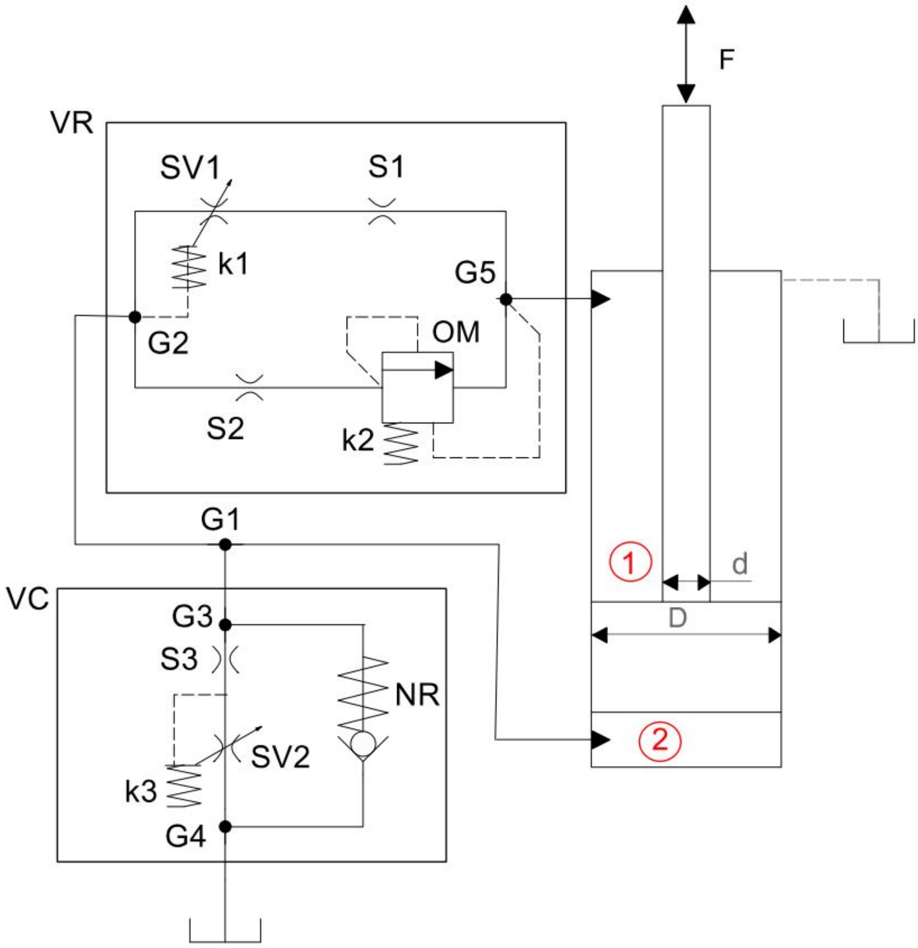

Figure 3.3: Damper hydraulic model schematics.

3.5 Compression phase

The compression phase is characterized by the downward piston displacement, it makes the pressure increase in chamber "2" and decrease in chamber "1". This difference in pressure is forcing oil to go from "2" to "1".The magnitude of the volume flow rate Q is obtained from the continuity equation of fluids and is directly proportional to the piston speed v.

$$Q = Av = \frac{\pi D^2}{4} v$$

The volume flow rate splits after G1 going toward G2 and G3. The magnitude of the two flows depends on the resistance encountered to flow in the relative branch. That resistance to the flow depends first on the characteristics of the restrictors S2 and S3, bigger flow area offers less resistance. If the condition of *minimum* is not exceeded, S2 and S3 transmit unchanged the pressure value to the following element, now the flow resistance is function of the two springs stiffness k2 and k3 that characterizes respectively OM and SV2 . If k3 is too low, it will permits oil flow to the reservoir earlier with respect to the requirement, leaving unfilled volume in chamber 1, that is not beneficial for the damper working. Therefore oil must go first to VR where the regulation of OM will control the flow. OM is sensible also to the pressure in chamber "1", with closing effect, therefore when the combined action of p_5 and k2 overcomes the effect of p_2, OM closes the passage not allowing oil flow. The pressure information is transmitted upstream to G1 and the volume flow rate in excess $\tilde{Q}$ coming from "2" is sent to G3, where it is disposed by the regulation of SV2 toward the reservoir.

$$\tilde{Q} = \frac{\pi d^2}{4}$$

3.6 Rebound phase

When the piston moves upward there is an increase of pressure in the chamber "1" due to the decreasing volume and simultaneously there is a decrease of pressure in chamber "2" due to the increasing volume. The pressure difference induces two distinct flows, one from "1" toward "2" passing through S1 and SV1 and the other one from the reservoir to "1"passing through VC. The total incoming flow to "1" is equal to Q and the flow coming to the reservoir is $\tilde{Q}$. It is important to guarantee the flow coming from the reservoir in order to avoid cavitation onset. During rebound phase the main parameter that control the operative point is the stiffness k1 because it is involved in the determination of the flow area. Then an other important characteristics required for the correct working of the system is that the preload of NR is sufficiently low to not obstacle the volume flow rate,

3.7 Compression valve

The task of the VC is already clear, now the focus goes on how it is made. In general the valve could be of the poppet kind, where the poppet closes the flow area pushed by the spring set-up with a certain preload for both the flow directions. But the trend is to use the shim valve kind instead of the poppet one for the oil flow directed to the reservoir. Shim valves are used in racing dampers for the simplicity in changing the characteristic and are used also on passenger cars dampers for the easy and consistent set-up. The check valve task for the back flow is often ensured by a poppet with annular shape. In the application used as example the shim valve is positioned within the poppet body as shown in figure 3.4. The assembly is composed by the following components:

- check valve seat;
- check valve body;
- screw and nut;
- carved disk;
- shims;
- conical spring;
- end-stop disk.

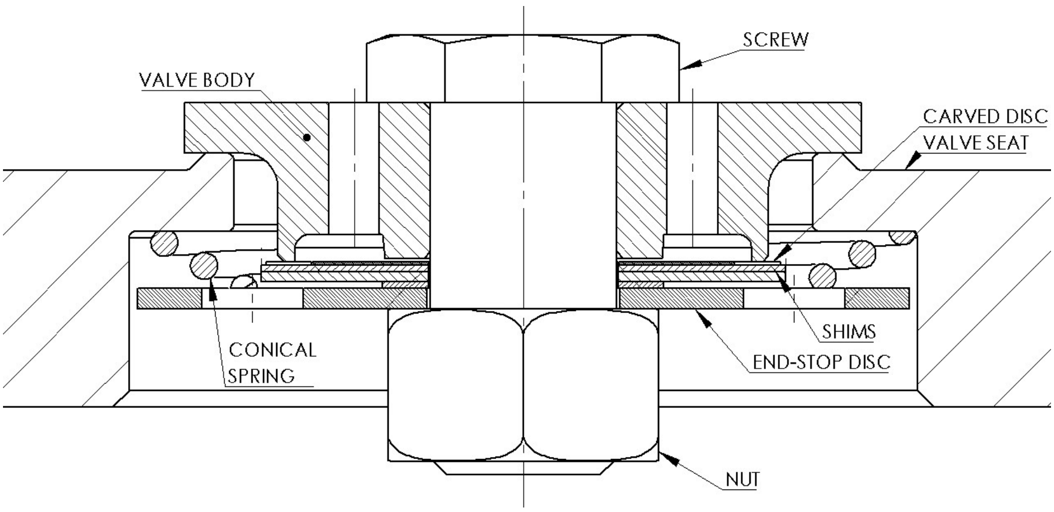

Figure 3.4: Compression valve section view.

The check valve body is provided by two holes, that in the schematics in figure 3.3 are modeled by the fixed restrictor S3. They are connecting the bottom chamber to the shims. The oil pressure acting on the carved disc is affected by the holes diameter in dynamic condition, because in static condition the pressure is transmitted by the fluid as stated by Pascal principle, but in dynamic condition the imposed volume flow rate is subjected to a pressure drop due to the orifice compensator behaviour. Therefore it is important to design the restictor not too small to avoid excessive pressure drop, not too big to limit the down-stream pressure in dynamic condition, to avoid shim damage under excessive pressure. In the example under investigation each hole has a diameter of 1.5 mm and their length is equal to 3.9 mm. First disc of the shim stack is carved to allow the volume flow rate pass also when the pressure is not sufficient to deform the stack, as during minimum flow, or in case of flow area obstruction due to external particles. The cuts made on the first shim are distributed symmetrically and in radial direction. In the example the carved disc has two circular shaped cuts with a diameter of 1.5 mm. That metallic disc has a thickness of 0.1 mm and a diameter of 15 mm. Compared to discs used in shim stack for VR it is smaller, that implies a higher bending stiffness for them and consequently a higher required pressure for the deformation that leads to increase flow area. The reason for this big difference in dimension can be the magnitude of nominal flow. The VR regulates the flow linked to one of the two active surfaces of the piston, instead the nominal flow of the VC is directly influenced by the rod diameter. The Valve characteristic is determined by the stack bending stiffness, in the figure 3.4 is shown the stack made by 3 discs, first one on the top is the carved one, the other two are solids with thickness of 0.2 mm and 0.3 mm respectively. In this case the three metallic discs have the same diameter, but generally they can have different diameters in order to satisfy the required bending stiffness characteristic. The stack hold its position by the compression action of the screw and the nut, in between there is the end-stop disc that has a double task, to limit the stack deformation imposing a maximum opening and to stop the poppet when back flow occurs. To distribute more uniformly the spring force, between the nut and the shim stack there is also a washer, furthermore it determines the maximum stack deformation with its thickness, because it is positioned between the end-stop disc and the shim stack. Last component of interest is the conical spring that holds in position the poppet. The main task of the conical spring is to limit the contact forces between end-stop disc and valve seat, when inversion of flow direction occurs. This valve has been chosen for illustrate the procedure to follow in order to compute its discharge coefficient by using numerical simulation.

3.8 Rebound valve

In this application the VR is using guided discs for the poppet task, their displacement is function of coil spring stiffness and of its active surface[2]. In fact when the valve is throttling, from the equilibrium respect to the axial direction the following equation comes out:

$$x = \frac{(p_1 - p_2)A - F_{preload}}{k}.$$

Where x is the poppet stroke, A is the poppet active surface, k is the spring stiffness, $p_1 - p_2$ is the difference of pressure acting on the 2 opposite surfaces. The flow path that the oil follows to cross the piston is obtained by circular holes with inclined axis. These holes are connecting the chamber at high pressure to the respective annular volume on the piston opposite surface. The components of the assembly are reported in the following:

- rod;
- piston;
- 2 coil springs;
- 2 guided discs;
- 2 spring supports;
- 2 depth rings.

The assembly has a sandwich organization, all the components are stacked on the rod threaded extremity with symmetry respect the piston in the disposition of the variable restrictor assembly, as shown in figure 3.6. The valve is crossed by the flow pushed by the piston itself. When the pressure difference is sufficiently high to move the respective guided disc, the cylindrical flow area increases allowing the working fluid to pass. The pressure threshold to start opening the flow area is set-up by the spring preload. Depending on the required damping behaviour the spring characteristic is chosen in terms of stiffness and prealod. The flow area has a cylindrical shape and it is obtained by the product of the metering edge circumference and the disc lift. The dimension of the flow area determines the working point of

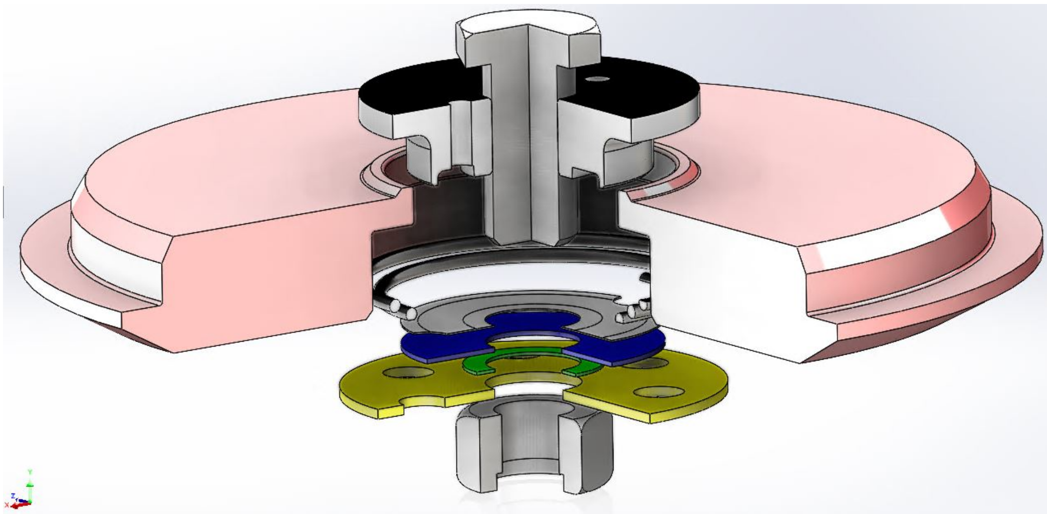

Figure 3.5: Compression valve exploded view.

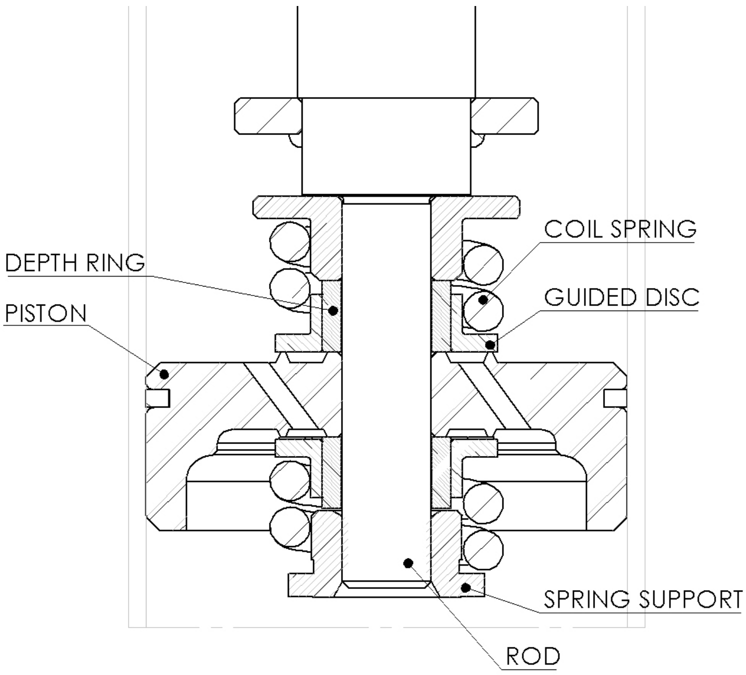

Figure 3.6: Rebound valve section view.

the valve in terms of pressure drop and volume flow rate. In order to have large flow area and volume flow rate due to small increase of pressure, a low stiffness spring can be chosen, leading to a smaller braking. Alternatively, if higher braking is required, it can be obtained by using a spring with higher stiffness. The piston is screwed to the rod threaded end, between the piston and each spring support there is a depth ring that constitutes the guide on which the respective poppet slides. The valve was modeled in the schematics of 3.3 using 2 branches in parallel, each one controls the flow in one direction. The top one ,where are positioned the fixed restrictor S1 and the variable one SV1, is in charge of managing the flow from chamber 1 to chamber 2. S1 represents the circular hole that connects two of the four annular volumes carved on the piston faces, two for each face. Downstream there is SV1 that represents the guided disc valve, where the coil spring stiffness is k1 and the active surface of the disc is subjected to the pressure difference across itself. The bottom branch instead manages the volume flow rate from chamber 2 directed to chamber 1, as well as for the top branch there are 2 lumped components, the fixed restrictor S2 and the relief valve OM. First one represents the circular holes as well as for the top branch, the second instead represents the guided disc assembly, where the spring stiffness is k2, also in this case the poppet is subjected to the pressure difference across it together with the spring force.

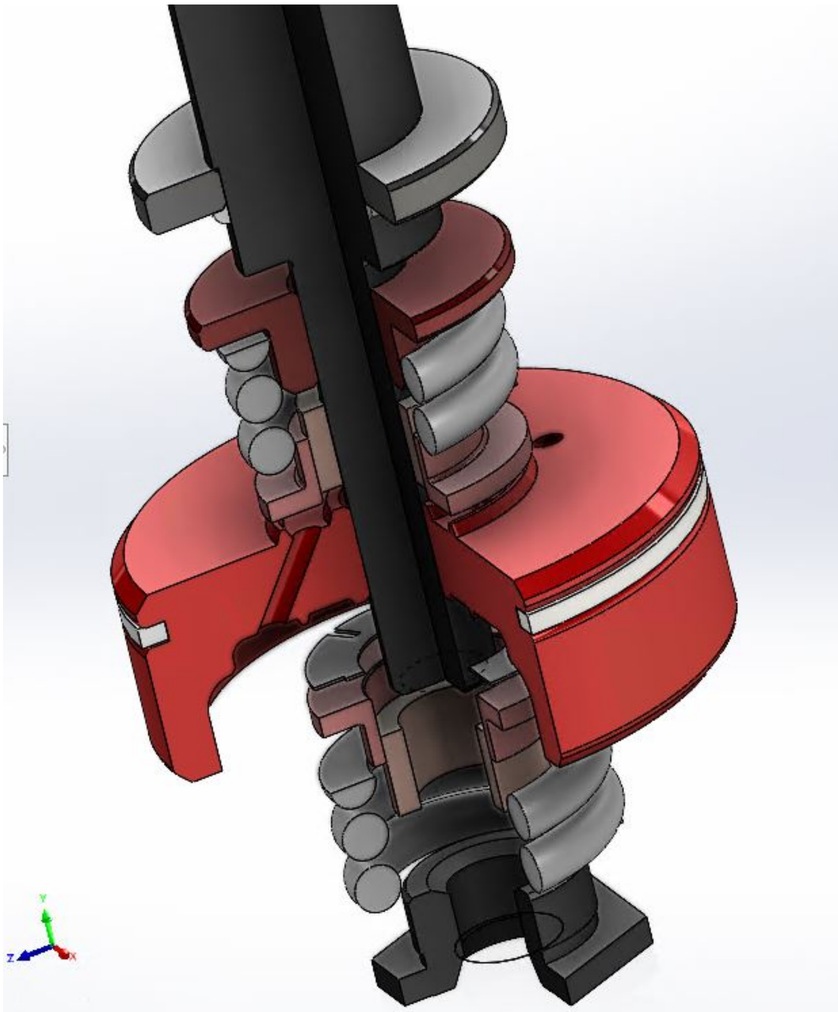

Figure 3.7: Rebound valve exploded view.

Part II

Simulations

Nowadays one of the most powerful tool for engineering are computer aided simulations, that offer the possibility to know the system behaviour before its manufacturing with a precision that depends on the accuracy of the model. This work wants to show the procedure to compute the discharge coefficient of a shim valve by using three typologies of simulations, with particular care about simulation cost, in terms of resources as time and computational power. First investigation carried out is about the shim deformation under oil pressure, it has been developed by using FEM simulation. Then the results that comes out are used to set-up the geometry for the second simulation step, where oil volume flow rate through the valve is investigated using CFD simulations. In the last step, the results coming from CFD are used to set-up the model developed on a power fluid software, in order to well approximate the corresponding discharge coefficient.

Chapter 4

Finite elements structural analysis

First procedure step uses the finite element modeling in order to compute the shim deformation under the oil pressure action. The analysis is carried out by using the simulation tool included in the Solidworks software, due to its intuitive organization and to its availability in the academic environment. In this chapter all crucial aspects of this tool are underlined, focusing on the simulation key parameters.

4.1 Shims

In order to investigate the valve behaviour, the attention goes on the shim stack. It has the task of controlling the flow area and it is sensible to the pressure drop across the valve itself. The flow area obtained by the stack deformation has both the behaviour of metering and compensator. In the initial phase the volume flow rate that should cross the valve is imposed by the piston speed, but the shims deformation is a consequence of the pressure drop across themselves. The pressure drop depends on the force imposed by the load and also by the shims deformation itself because it determines the passage area of the flow that has an influence on the upstream pressure. Due to that mutual interaction, dividing causes from effect can be difficult. To overcame this issue some considerations are made determining unequivocally the path to follow. The cause of the deformation is for sure the differential pressure across the active surface, therefore this is the starting point in order to characterize the shim stack. Imposing the pressure on the active surface for that structural analysis gives as output the corresponding deformation. That analysis is developed in static condition under the hypothesis of slow deformation. This condition is far from the reality, due to all non linearity involved, but still reliable for the required output. Increasing gradually the pressure on the shim active surface and collecting the corresponding deformation, comes out the shim pressure-deformation characteristic. By using geometrical considerations it is possible to compute the flow area starting from the deformed shape obtained by the FEM analysis, that will be used after, when it will be the turn of the lumped parameter simulation. The stack can be composed by several discs, in this application it is made by only 2 discs, due to the small dimensions, plus the washer used to better transmit the screw compression force, that does not deform. The first disc of the stack is carved to ensure the minimum flow area, it has a thickness of 0.1 mm and a diameter of 15.5 mm. Second disc has the same diameter of the first one but it has a higher thickness, its value is 0.2 mm. The CAD model of the stack is represented in figure 4.1 with isometric section view. The carved disc is the one colored in lilac, the second one is colored in blue and the

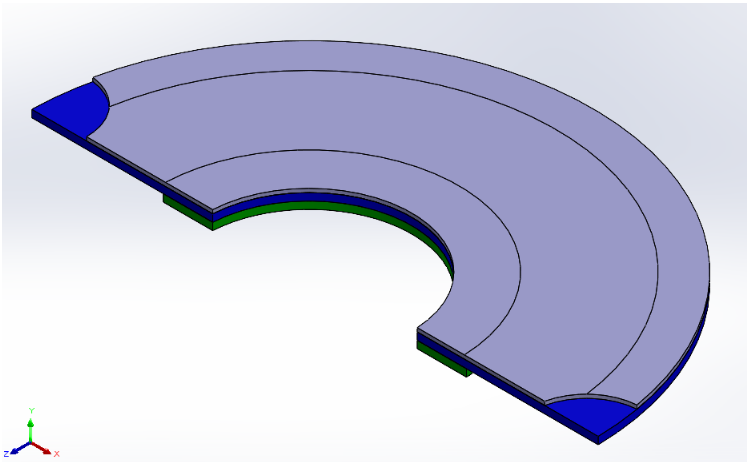

Figure 4.1: Shim stack section in isometric view.

washer is the green component. On the top surface of the carved disc are visible 2 concentric circumferences, the annular surface delimited by the two ones represents the active surface where oil pressure acts. In fact the inner line is in correspondence of edge around which the disc bend and the outer one correspond to the metering edge of the valve. The stack is mounted with certain preload that depends on the difference in height between the 2 surfaces of the valve body where the top disc goes in contact. The higher the the difference the higher the preload, in this example the height difference is about 0.1 mm. FEM simulation are carried out starting from the undeformed shape, therefore when the flow area consequent to a determined deformation of the stack is computed, it must be corrected by a factor that takes into account the preload. One of the fundamental aspects for structural simulations is the material definition. The shims are made in steel, but on the market there are thousand of different kind of alloys. To investigate the behaviour of the real product performance is out of the scope of this work, that focuses instead on the procedure to follow in order to compute the discharge coefficient of the shim valve. Has been chosen therefore one of the material available on the software database, in particular the steel AISI 4340 normalized. Its main characteristics are listed in the table 4.1. This material has been selected for the high value of the yield strength and it has been assigned for both the discs and washer. In the reality they can be made with different materials. The right material for the right application needs to be used.

In this case the deformation of the object is high compared to its dimensions. At the maximum opening configuration of the valve, high level of stress can be reached, therefore the material must be chosen with care in order to avoid overcoming the yielding strength, avoiding the possibility of plastic deformations during working.

Table 4.1: AISI 4340 steel: material characteristics.

Property	Value	Units
Elastic modulus	205,000	MPa
Poisson's ratio	0.32	-
Mass density	7,850	kg/m^3
Tensile strength	1,110	MPa
Yield strength	710	MPa

4.2 Contact

During simulation set-up, the kind of contact between the discs must be defined with respect to the nature of the physical problem. The used software offers three options to model the typology of contact constraint between two surfaces in touch, figure 4.2 summarizes them.

- Bonded: selected surfaces can not move with respect to each other, therefore the two components behaves like a unique body, as if they were welded.
- No penetration: this contact type prevents interference between two bodies but allows gaps to form. This option is the most time consuming.
- Allow penetration: this option treats the two components as disjointed. The loads are allowed to create interference. This option is time saving with respect to the other two, but in order to be used requires absolute certainty of no interference.

The type of contact can be defined for the total assembly or more specifically between the two components surfaces in contact of the assembly. First method is more time consuming due to the fact that the software has to search for the contact region by itself. In this case the assembly is small, being made by only 3 components, and the surfaces in touch are recognized easily, therefore the only the global contact was set without specifying it for each couple of joined surfaces. Regarding the analyzed application, no penetration typology of contact was selected. Because the other two do not model in the correct way the type of interaction. If option bonded is chosen, the solids behave as one, not admitting relative sliding between the surfaces, and therefore a consequent overestimation of the stiffness. On the contrary, if allow penetration option is chosen, the solids behave as if they were completely separate, not allowing interaction between the surfaces, and therefore a consequent underestimation of the stiffness. After the choice of the no penetration option, the

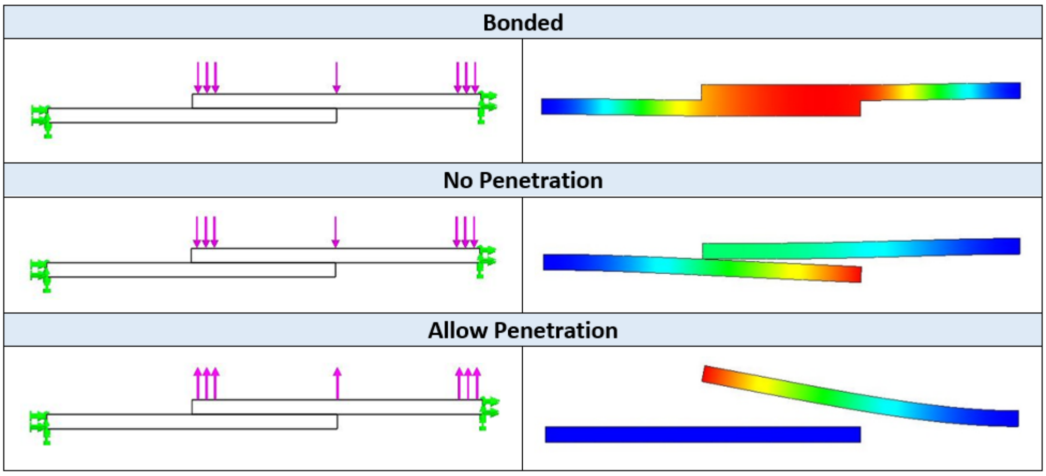

Figure 4.2: Contact options.

friction coefficient between the interested surfaces needs to be defined. In this way the contribution coming from the friction is taken into account, giving a more reliable solution. For this group of simulations the value of the friction coefficient that has been chosen is 0.08 referring to lubricated good finishing surfaces made in steel.

4.3 Constraints

Next step in the simulation set up consist into the definition of the external constraints. The stack is clamped between the washer and the valve body by the compression force transmitted by the bolt. The screw behaves as a spring under traction. This force is directed along the screw axis and in magnitude depends on the screw material and tightening torque. The effect of this bolted joint is the locking of the stack in the region in between the washer and the respective surface of the carved disc. The washer diameter is about 8.3 mm. Its external edge in contact with the bottom disc fixes the circular area around which the disc is bending. The same happens for the top disc around a circumference with a diameter of 8.18 mm, that correspond to the surface of the valve body coupled with the top disc. The effect of the screw force is not only the locking of the stack in the vertical translation, but also the locking of the other 5 degrees of freedom. Thanks to the friction between the respectively joined surfaces, a certain friction force in the radial direction arises, that holds in position the entire stack. For the simulation set-up therefore has been chosen to apply the fixed constraint to the interfacing surfaces. Also the internal cylindrical surfaces of the discs were constrained in all the 6 degrees of freedom, in order to avoid that the total reaction force is beared by the two interface areas, because it could lead to wrong results. The 2 diameters mentioned previously have an important contribution when computing the bending stiffness of the stack. If they were smaller, the disc would have been loaded by a higher total force, given by the product of pressure and active area. Furthermore, for a structure subject to bending, the main length has an effect on its stiffness. The greater the length, the smaller the stiffness. Hence to a smaller circumference around which the disc bends corresponds a lower bending stiffness. In figure 4.3 the constrained surfaces were underlined in cyan.

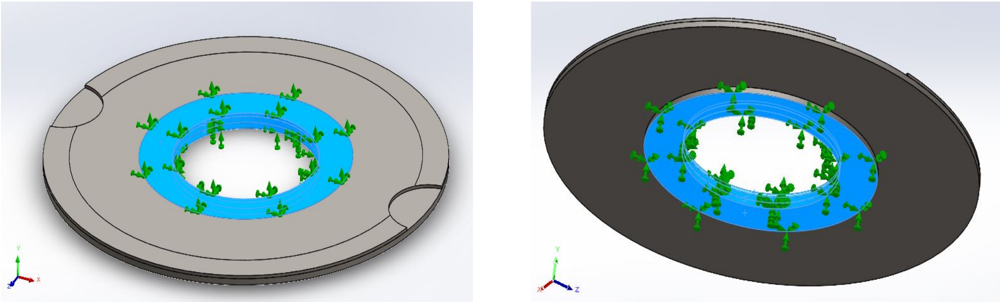

(a) (b)

Figure 4.3: shims stack constraints,(a)top view, (b) bottom view.

4.4 Loads

As already said, the stack deformation is the effect of the oil differential pressure between the disc top surface and the bottom one. On the annular area acts the normal pressure equal to the one downstream the fixed restrictor S3, that represents the two circular holes crossing the valve body. On the bottom surface is acting the pressure level of the reservoir, that is at environmental pressure. It is reasonable to consider only the relative pressure on the top surface instead of the differential one. To specify the region where the load acts, the top surface of the carved disc has been divided in three annular areas by two concentric circumferences, with a diameter of 8.18 mm and 15.5 mm respectively. The division was performed by using the command *splitline*, it is helping making the selection faster and accurate. Furthermore the software will recognize the lines as reference for the mesh generation, that will be compatible to the geometry in that particular regions. In the reality the pressure that acts on the annular area do not have a constant distribution, the volume flow rate that crosses the valve is not supersonic, therefore the downstream pressure can influence the upstream one going up the stream. Moreover the total pressure is given by 2 contributions, the static one and dynamic one. Increasing the flow speed, according to the Bernoulli's relation there is a decrease of the pressure. The volume flow rate accelerate in the restricted section, this is a corollary of the continuity equation for fluids. Therefore it is acceptable to consider loaded only the central annular area, due to the big pressure reduction after the metering edge. As first approximation the pressure that deform the shim stack is considered constant and uniformly distributed, in order to simplify the computation, but for future development the simulation can be refined by using a non constant distribution of the pressure, that mirrors the reality of the phenomenon. In Figure 4.4 is underlined in cyan color the surface where the pressure acts. Four load steps were tested, with a pressure of 22 bar, 25 bar, 27 bar, 30 bar.

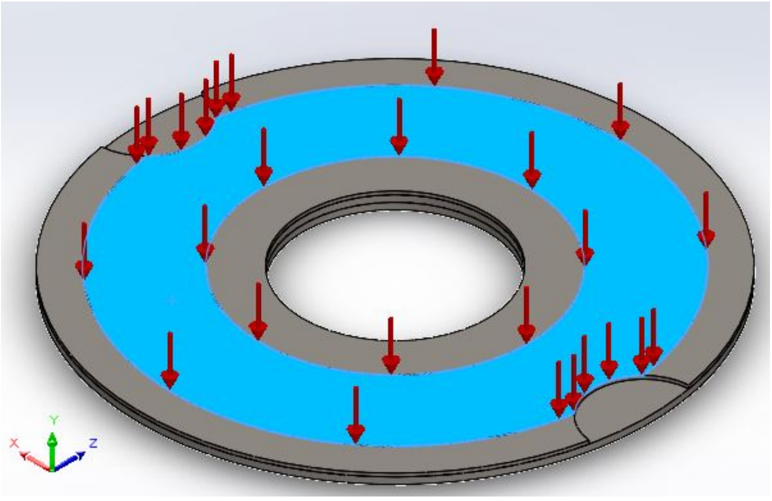

Figure 4.4: Pressure on top shim active surface.

4.5 Mesh

Speaking about mesh in FEM environment, means the level of discretization by which the solid body is divided. It has severe effects on the simulation results, an higher refinement level leads to more accurate results, but the time required for the simulation completion increases too, maintaining unchanged the computational power. Therefore it is convenient to perform a mesh sensitivity analysis, where the mesh is progressively refined collecting the respective results about a target parameter and the required computational time. In this way the variation associated to the target parameter can be compared to the time required to terminate the simulation. Then the analyst will choose the appropriate trade-off in terms of accuracy and timing. The dimension of the discretization element is not the only one parameter that affects the result accuracy. It is important to keep attention to the kind of element chosen. It is possible to distinguish 3 main categories of element regarding its predominant dimensions. If one dimension is ten times bigger than the other two, it is the case of 1D elements, like rod or beam. When two dimensions are bigger than the third one is the case of 2D elements, like membrane or shell. If the element has comparable dimensions in all the three directions, it is the case of 3D elements. Second possible difference is about the direction of the applied load, for example if it lies on the plane containing the element or if the load can be perpendicular to that plane. Further each element can be discretized with more than the strictly necessary nodes, resulting in a more accurate result. The software used to develop the simulation offers three types of mesh, solid tetra,triangular shell and beam. It automatically recognizes the most appropriate element to use. According to what has been described previously,the most appropriate type of element to discretize the discs seems to be the shell one. But due to the discs small dimensions, solid mesh is automatically chosen by the software. In order to choose the element dimension mesh sensitivity analysis has been performed, where the target parameter is the deflection in correspondence of the metering edge, the element characteristic dimension is progressively reduced starting from a value of 0.6 mm and the load is maintained constant for each simulation with a value of 25 bar . Figure 4.5 shows on the left hand side the coarser mesh used for the analysis, corresponding to the characteristic dimension of 0.6 mm and on the right hand side the level chosen for the total number of structural simulations, corresponding to an element characteristic dimension of 0.2 mm. Figure 4.6 shows a zoom of the finest mesh used for the analysis, to which corresponds a model composed by 235,530 elements. The analysis results

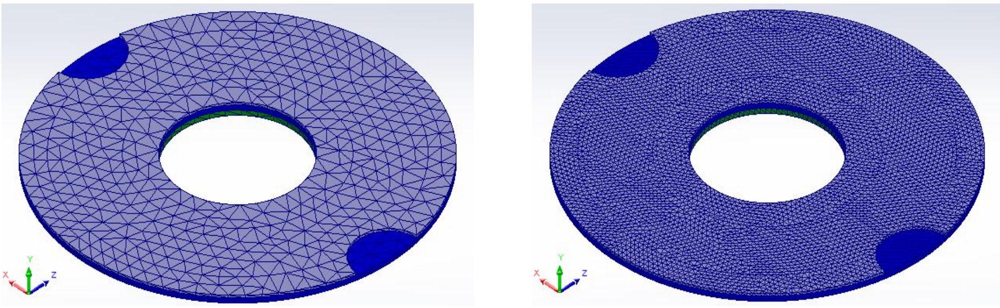

(a) (b)

Figure 4.5: Different mesh refinement level,(a)coarse, (b) fine.

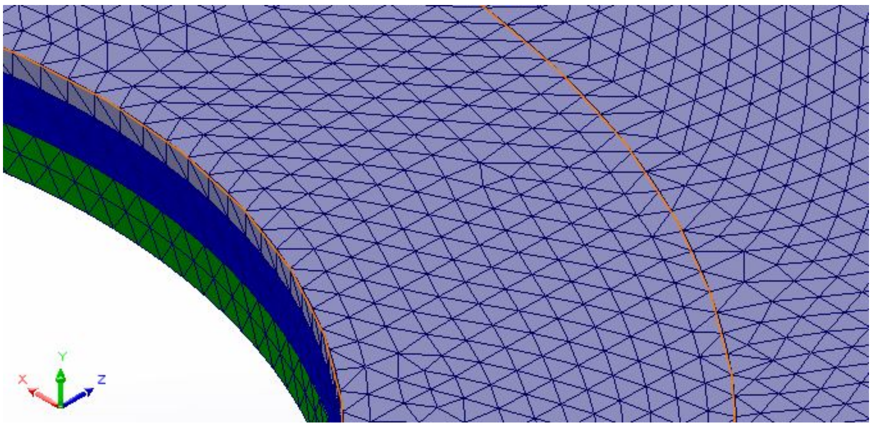

Figure 4.6: Zoomed view of the finest mesh used for the analysis.

are summarized in figure 4.7 where two plots are showed. The red one represents the trend of the deflection, associated to that load, increasing the number of elements. Using coarse mesh the approximation error of the simulation results can be high. Going on with the mesh refinement the resulting deflection shows a stable trend. In blue is plotted the curve of computational time vs number of elements. It shows an increasing trend, as expected. Using more than two hundred thousand elements the computational time required to complete the simulation is around 3 hours on a four-core Xeon 3550 processor at 3.06 GHz and the resulting deflection is 0.114 mm. Instead using less than one hundred thousand elements the required computational time is around one hour and the simulation result is 0.1152 mm. The difference between that two results is around 1% saving about two hours. Then the mesh configuration with a characteristic dimension of 0.2 mm, to which corresponds a finite element model composed by 68,546 elements, was chosen to perform the rest of simulations used to study the deformation behaviour.

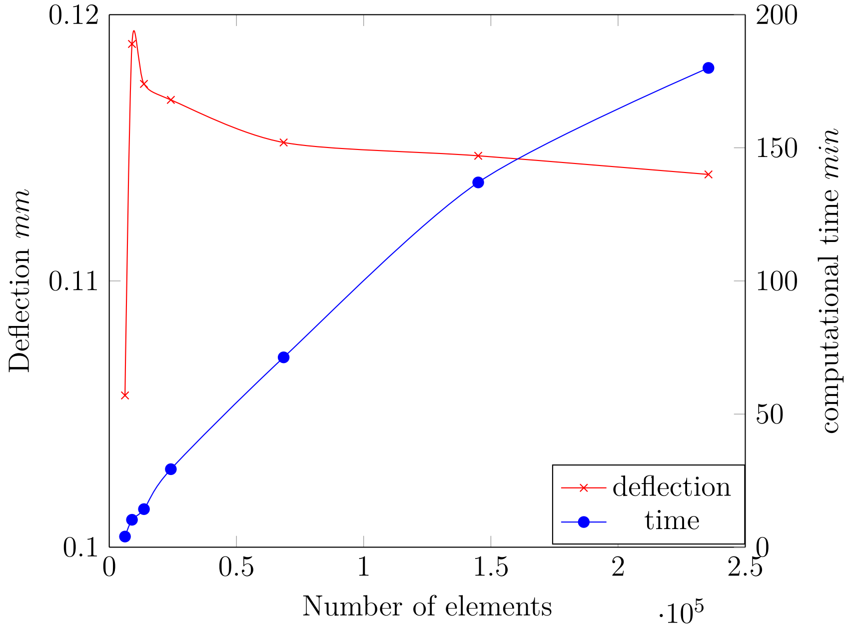

Figure 4.7: Mesh sensitivity analysis results.

4.6 Results

Structural simulations were performed using the previously described model. Each simulation differs from the others by only the applied level of pressure. As already said, the shims stack has a certain preload, therefore the superimposition of effects is considered. The height of the cylindrical surface corresponding to the flow area is computed by subtracting the preload distance to the simulation result. The shape of the flow area is not perfectly cylindrical, the effect of carves on the top discs can be modeled adding two rectangular surfaces to the cylindrical one. The valve operative range depends on material and number of shims composing the stack. Flow area is progressively increased after that the preload equivalent pressure is overcomed. For the analyzed configuration, in terms of material and number of shims, the cylindrical surface starts to increase around 22 bar, and the maximum opening is reached around 30 bar, when the bottom shim goes in contact to the limiting disk. Four levels of pressure have been tested and their results are shown in figure 4.8, where the average deflection in correspondence of the metering edge is plotted. To obtain the real displacement between top disc and metering edge, the value of 0.1 mm, corresponding to the preload distance must be subtracted. The plot shows a linear trend as if the elastic member was a coil springs, but in the reality the behaviour of shims under bending is not linear. The evaluation of the deflection for each level of pressure was performed averaging the displacement in the vertical direction for all the nodes positioned in correspondence of the metering edge. Figure 4.9 compares the results of the simulations performed in the configuration of minimum opening and complete opening, respectively with a pressure level of 22 bar and 30 bar. Looking to the left hand side picture it can be notice that the vertical displacement of the shims is not axial symmetric, it is bigger in the zones away carves. This behaviour is due to the presence of carves, they reduce the surface where pressure acts and they also increase the local bending stiffness due to the smaller radius.

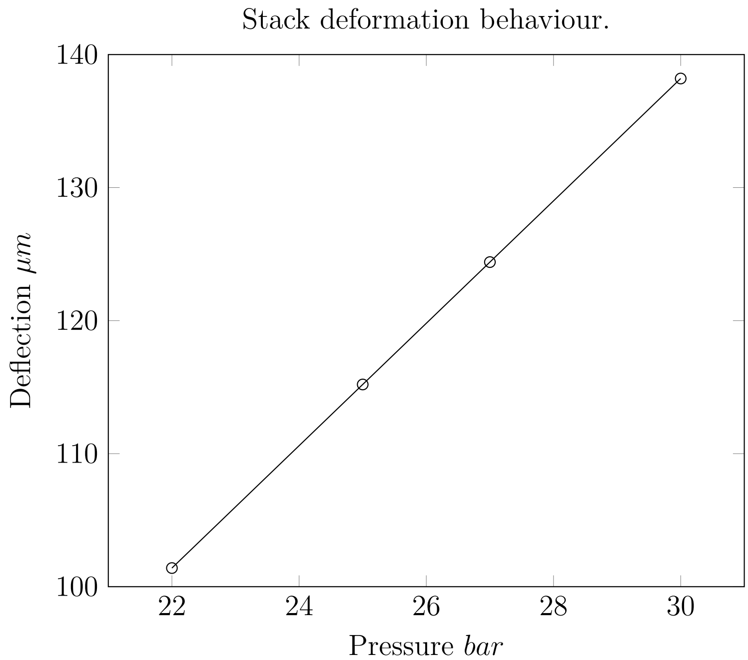

Figure 4.8: Static structural simulations results.

The deformed result has been plotted with a scale factor equal to 10, in order to underline the deformed shape. The scale of the contour plot was set equal to better show the differences between the two load cases. The scale goes from red to dark blue. Due to the chosen reference system the vertical displacement has negative sign, red color is associated to the maximum displacement, that in this case can be considered equal to zero. In fact the deformation in the red zone is only due to the compression state when the valve is assembled. The regions colored in blue are the ones at minimum displacement, that absolutely speaking instead corresponds to the maximum deformation. The two compared results shows a similar deformation behaviour. Instead regarding the maximum stress reached in the structure, as expected, it is higher in the maximum opening configuration. Where it overcomes the yielding limit of the selected material. Figure 4.10 shows the stress distribution on the top surface of the thicker disc, computed using VonMises definition, with the 30 bar load. In the reality this issue can lead to valve malfunctioning, but the structural integrity of the valve is out of this text objective, therefore only the deformation values are used to go on with the investigation of the valve discharge coefficient. The problem of structural integrity can be fixed by changing the shims material or the number of discs composing the stack, but both solutions are influencing the operative range of the valve, with consequences on the damper braking behaviour.

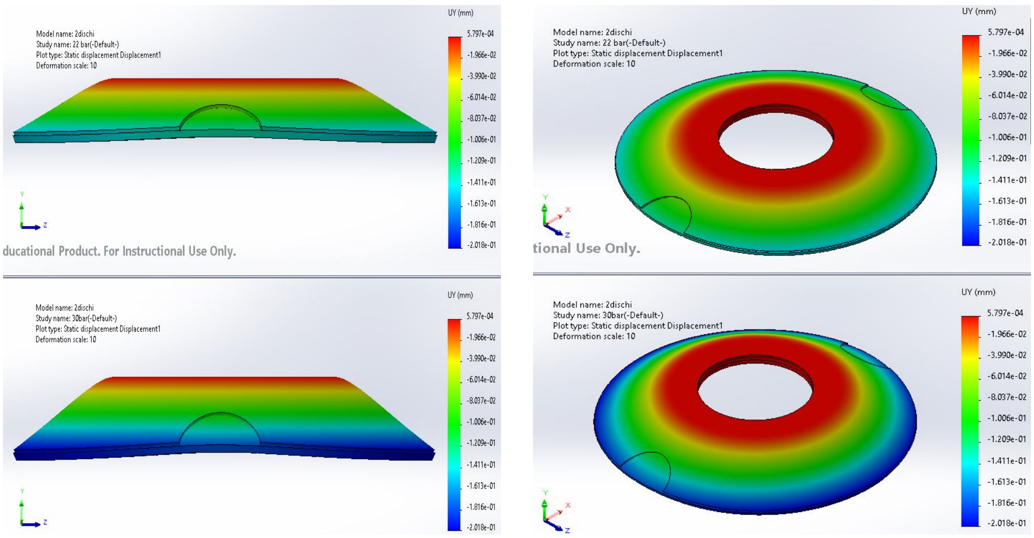

(a) (b)

Figure 4.9: Simulation results comparison,(a)lateral view, (b) isometric view.

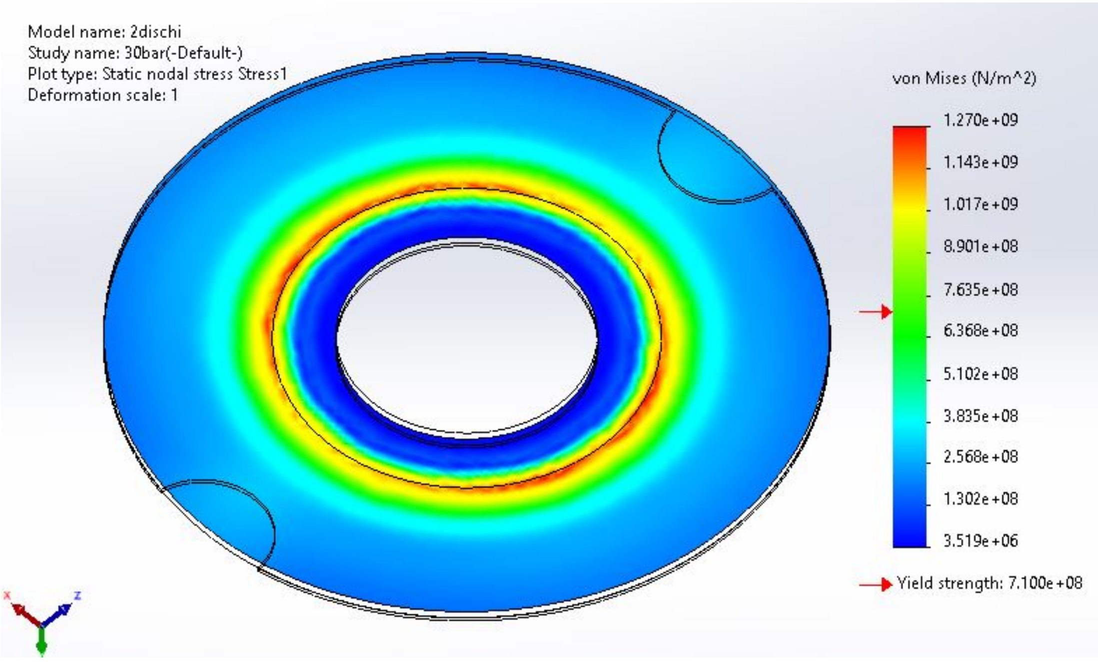

Figure 4.10: VonMises stress distribution on second shim top surface.

Chapter 5

Computational fluid dynamics

The second step, in order to obtain the valve discharge coefficient C_d, consist in the computation of the volume flow rate Q_{VC} associated to each value of the pressure drop across VC. The $p - Q$ characteristic of a generic orifice can be analytically computed for simple geometries, when C_d, working fluid properties and flow area are known. In this case the valve geometry cannot be considered simple and analytic formulas are not sufficient. Therefore, to compute the $p - Q$ characteristic, numerical methods are required. Computational fluid dynamics simulations approximate with a certain reliability the working fluid behaviour under defined boundary conditions. This method consists in three phases: pre-processing, solver run, post-processing. First phase consists in the domain discretization, by dividing the fluid volume in cells and the solid boundaries in a compatible way. Then the CFD model is completed with the boundary conditions definition. Second phase is carried out by the software called solver, where fluid constitutive equations are solved iteratively for each fluid cells until the convergence is reached. The last phase consists in the results visualization through graphic tools that make understandable the fluid behaviour. In this chapter is described the investigated methodology for the CFD model preparation of a shim valve, when computational resources are limited. Then simulations results are presented and compared, to underline their differences due to model set-up properties.

5.1 Model introduction

Before to set up the CFD simulation, it is required to determine the environment where the oil is flowing by the definition of the geometry. To each value of the upstream pressure corresponds a certain shim stack deformation, as was previously established through the FEM analysis. Therefore only one geometry model is not sufficient for testing the valve in the whole working range. The geometry of the model has to be updated or modified according to the results coming from the structural analysis. The start point is the CAD model of the valve. Using the tools included in the engineering software, it is possible to create a new part with the shims deformed resultant geometry. Then a new assembly is modeled where the CV CAD model is used, by substituting the shim stack components in the undeformed configuration with the deformed result. Proceeding this way it is required to prepare one model for each level of pressure that has to be tested. The major constraint in the developing of CFD analysis is the maximum number of cells that can be used to discretize the fluid domain. That limit is set up by the dimension of the random access memory that is equipping the machine used for the computation. Generally to solve this kind of analysis using Solidworks are required 3 Gb of memory for each million of cells, but more professional software packages requires 1 Gb for each million of cells. The maximum number of cells is therefore limited by the machine hardware from the technological point of view, but it is also limited in its minimum number by the geometry that is going to be tested. In order to model correctly the fluid behaviour when it is flowing inside a channel, it is required to have more than ten cells along the direction of minimum distance. The fluid speed for example is not constantly distributed inside a channel, but it is higher far away walls and lower closer to the walls. Using too few cells in modelling a channel can lead to wrong results. Due to that reason, the most critical case between the analyzed configurations is the one with minimum flow area. Because it requires mesh with a higher level of refinement, that implies a higher number of cells. All the analyses have been performed on a machine equipped with a 12 Gb RAM, of which only 10 available for the computation. The maximum number of cells that can be used is therefore around 3 millions. By using the above described procedure for the geometry set up, is almost impossible to create a CFD model that ensures all the requirements. Therefore geometry simplifications are performed and their effect is investigated for less critical configurations, then the best compromise in terms of accuracy and timing is extended to critical cases. Geometry simplifications are intended on 2 levels. It is possible to rebuilt the total environment maintaining unchanged main details and study only a part of the model under the definition of characterizing symmetries. Or instead a new model can be built where only a part of the original model is considered. Then the total objective is computed by adding all the contributions. First attempt has been made on the full assembly model, where the deformed shims configuration is imported. Then the symmetric model has been tested, where the geometry has been simplified by the realization of a new model that in only one component reproduces the characteristics of the valve in a determined configuration. Unfortunately the previous simplifications were not sufficient and a third kind of model has been tested, the slice model. Where instead of the total model, only a slice is analyzed. In this study, thermal aspects are neglected by setting ideal adiabatic walls condition. The valve under investigation has an intrinsic temperature dependency due to the properties of the working fluid that are function of the temperature. The energy dissipated by the damper is transformed in heat, that makes oil temperature increase, an other task of the reservoir is in fact to cool down the working fluid by the exchange of thermal energy with the external environment. But in this work temperature has been considered constant, therefore also the oil properties that are function of it will not change. The fluid minimum pressure has been limited by enabling the cavitation option, to model appropriately the physical phenomenon involved. The flow surface is really narrow in the first opening phase, due to the sharp geometry and the environmental pressure downstream of the reservoir, there is the risk of cavitation. Furthermore an overestimation of the pressure drop across the valve can lead to a wrong volume flow rate computation. The target of performed simulations is the estimation of the volume flow rate that crosses the valve for each level of pressure tested, in order to fully characterize the CV hydraulic behaviour.

5.2 Working fluid definition

Before to describe the different kinds of models tested, it is good to define the characteristics of the working fluid. Dampers generally use oil as working fluid for its characteristics. In fact oil has optimum lubricating properties and it is characterized by its viscosity that has a role in the energy dissipation process. The viscosity is a function of the temperature, the higher the temperature the lower the viscosity. Density too has a variation with temperature, but this dependency is less critical than the one of the viscosity. Oils designed for dampers purpose are blended with additives in order to avoid steel components oxidation and to enhance lubricating properties. The characteristics of the working fluid used for all the CFD simulations come from the product data sheet of a famous european enterprise that has as core business oil for mechanical purpose. Oil characteristics of interest for the objective of this text are summarized in table 5.1. The trend of the viscosity vs temperature for oil is

Table 5.1: Oil properties.

Property	Value	Units
Density @ 15°C	826	kg/m^3
Kinematic viscosity @ 100°C	5.7	mm^2/s
Kinematic viscosity @ 40°C	28.1	mm^2/s

generally a branch of hyperbola, but due to the lack of data it is considered constant and equal to the value corresponding to 40°C, because the procedure investigation is not depending on specific data used, but more on which strategic decisions can make the computation easy and faster.

5.3 Full assembly

First attempt has been performed by using the shims deformed shape imported from the FEM simulations result. This method of defining the model geometry is the one that requires less time in terms of model preparation, but it is affected by some issues. It includes regions where fluid behaviour is not of interest for the developed analysis, this makes heavier the model by increasing the total number of fluid cells. The software used for the developing of the analysis selects the dimension of the cells starting from the main dimension of the control volume, in order to set-up hexahedral cells as regular as possible. Therefore starting from a bigger volume, it is required to perform higher refinement with respect to the case where the control volume is smaller, when discretizing a particular fluid region of interest. The region of most interest for the characterization of the valve is the annular volume where the pressure drop is concentrated. It coincides with the space in between the valve body and the top shim. In this region the mesh must be enough refined to correctly model the flow behaviour. This can make the total number of cells increase too much, resulting in a model that can not be solved with the available resources in terms of hardware. Another problem related to the full assembly model is the presence of gap between shims surfaces, where generally there is no flux, but they are included automatically in solver computation, increasing time required to perform the simulation. The full assembly model has also some pros, in fact the deformation of the shims is not axisymmetric, as it has been described previously, but it is higher far away the carves obtained on the top disc. Therefore this model gives a more realistic characterization, representing in total all the different details affecting the valve working. The main characters of the model are presented in the following sections.

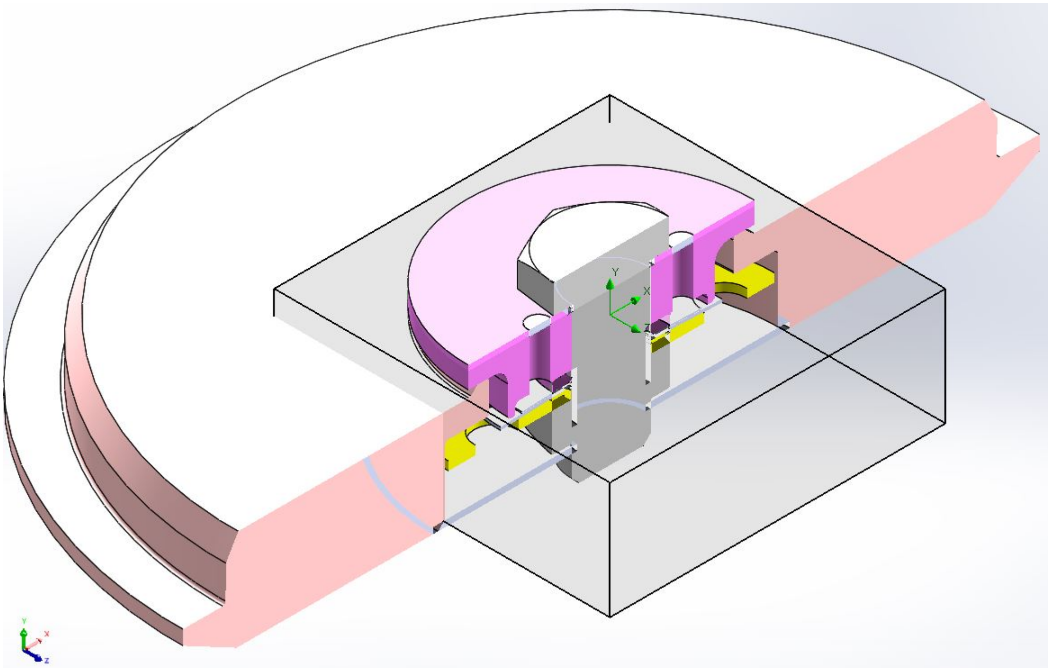

Figure 5.1: Full assembly CFD model in section isometric view.

5.3.1 Components

The assembly components are the original CAD models of the elements that assembled constitute the CV, minus the shim stack that is substituted by its deformed configuration imported after the finite elements analysis. Those items are not sufficient for the model set-up, other particular bodies are added to the assembly in order to define the regions where mesh is going to be refined. Such items are included to the model as solid bodies and then are disabled through the components control window. In that way the fluid is not interacting with those elements because they are not considered solid bodies. Two bodies have been modeled, one with the task of representing the metering volume in the restricted section, the other one to define the volume of interest in the carved region on the top disc. Each one of them is used twice in the full assembly model, to define the volume of interest all around the metering edge that has a circular shape. In order to perform the internal CFD simulation it is required to seal the model by the use of lids. They are caps that are closing the intake channel and the discharge one. Their internal surfaces are used to set-up the boundary conditions for the simulation. Lids are created by selecting the planar surface that needs to be closed, automatically the software recognizes the opening, it completes the task by the generation of this new bodies fundamental for the tight seal condition set-up of the model.

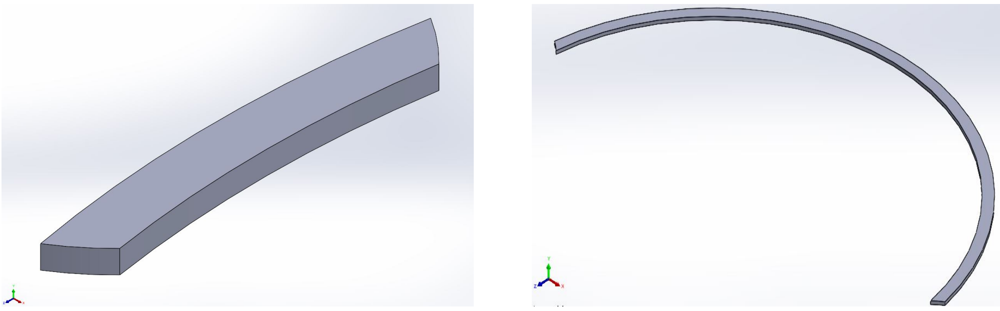

(a) (b)

Figure 5.2: Extra components used to define mesh refinement regions,(a) carved region, (b) restricted region.

5.3.2 Boundary conditions

After the geometry definition it is required to set-up the boundary conditions. The goal of the simulation is to compute the volume flow rate that crosses the valve with respect to the upstream pressure. Therefore the intake surfaces are set at the upstream pressure that is going to be tested. Instead the downstream boundary condition is set on the bottom lid, on the surface that virtually closes the valve, dividing the fluid volume from the rest of the reservoir. The boundary conditions are completed by the setting of the simulation goal. It is defined as surface goal by selecting the internal surface of the intake lid. Because the volume flow rate is computed starting from the surface crossed by the fluid flow. The goal convergence is considered as criteria for the the simulation finish. Figure 5.3 shows a section of the model where are underlined the boundary conditions.

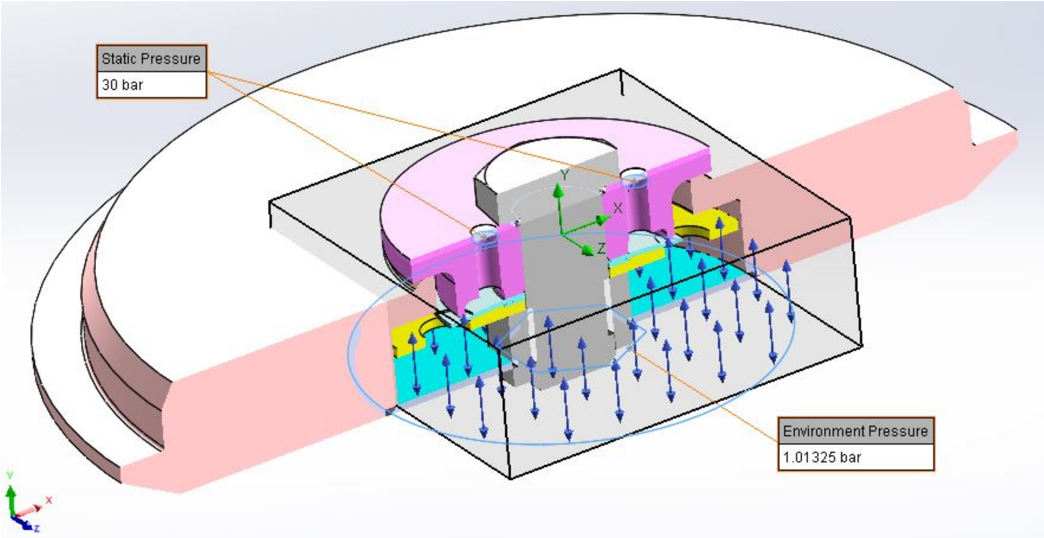

Figure 5.3: Full assembly CFD model in section view with boundary condition in evidence.

5.3.3 Mesh

The most critical part of the model preparation consists in the subdivision of the fluid volume in cells. This procedure has the major contribution in the result accuracy. The maximum number of cells is limited in total by the available computational power. Locally instead the minimum number of cells is limited by the channel geometry. The smaller the gap, the higher the required mesh refinement. The situation changes with respect to the upstream pressure, when the valve is in the minimum opening configuration, the gap is really tight. Instead in the maximum opening configuration the channel to refine is enough big to do not cause critical issues. For these reasons it was not possible to make a model using the total assembly method for all the opening configurations by using the available computational power. Only the maximum opening configuration has been tested. However in order to test the other configurations that are more critical for the mesh generation, new models have been created, where under symmetry assumptions, the geometry has been simplified in order to better catch the requirements. Figure 5.4 shows an enlargement of the mesh in the areas of interest, respectively the restricted one in the left-hand side and the carved one in the right-hand side. Figure 5.5 instead shows the mesh refining plot for the entire valve in correspondence of the X-Y plane.

5.3.4 results

Several attempts of the simulation run have been made, using different mesh configurations. The parameters on which it is possible to play with mesh are three, the global refinement level and the local refinement level in the 2 regions of interest. For

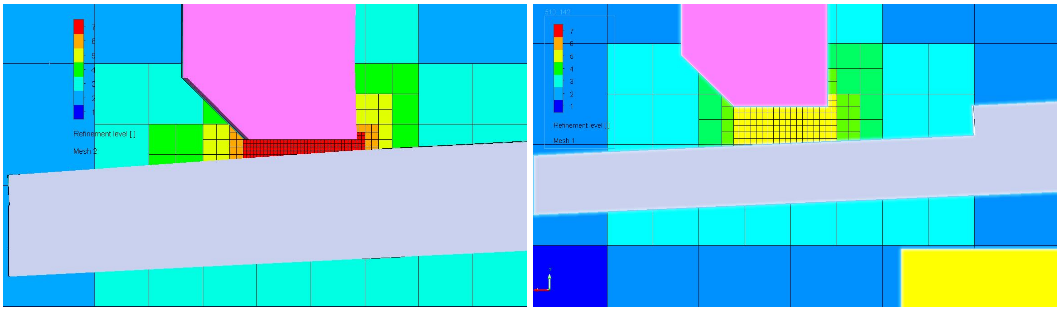

(a) (b)

Figure 5.4: Full assembly model mesh refinement ,(a) restricted region, (b) carved region.

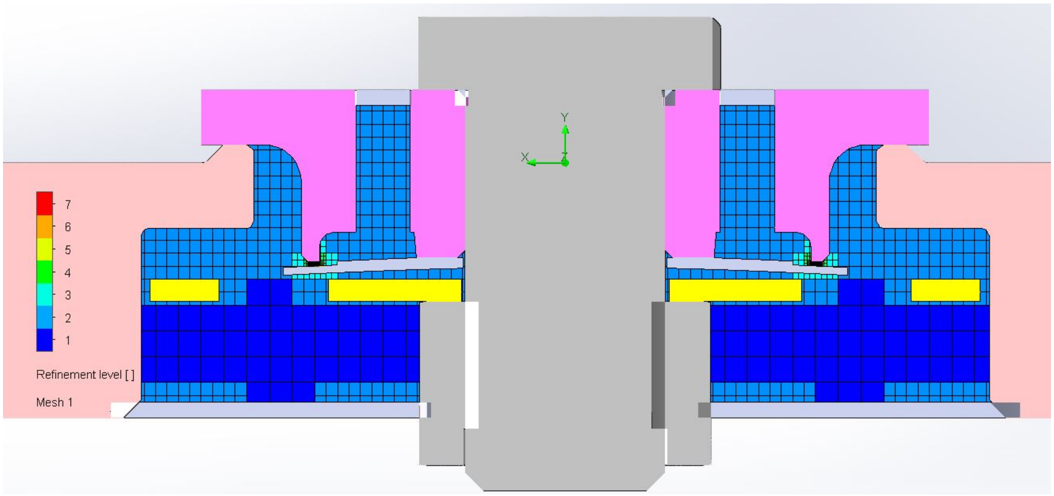

Figure 5.5: Full assembly mesh cut plot.

the carved region, to achieve enough refinement was not difficult due to the big dimensions of the channel of interest. Instead for the restricted section case was more difficult to fulfill the requirements in terms of channel refinement due to its small dimensions. By increasing the refinement of 1 level, the total number of cells included in that region became 8 times bigger. This system of refinement puts a limit on the maximum number of cells that can be used to discretize the fluid volume. However the information that comes out after all the attempts is the mesh refinement influence on the S3 restrictor. Because using low refinement in that region, in order to increase the number of cells in the restricted region, gives a resultant volume flow rate not in line with the other attempts, where higher refinement has been set for the global mesh level. Discretizing the volume passing for S3 in raw way has directly influenced the results, due to that in the next models the S3 restrictor will not be included in the model, focus the effort on the metering region effect. Using a mesh composed by around one millions of cells the resultant volume flow rate associated to a pressure drop of 30 bar was around 6.6 l/min. Figures 5.6 and 5.7 show respectively The pressure cut plot for the carved region and the flow trajectory as function of the fluid speed.

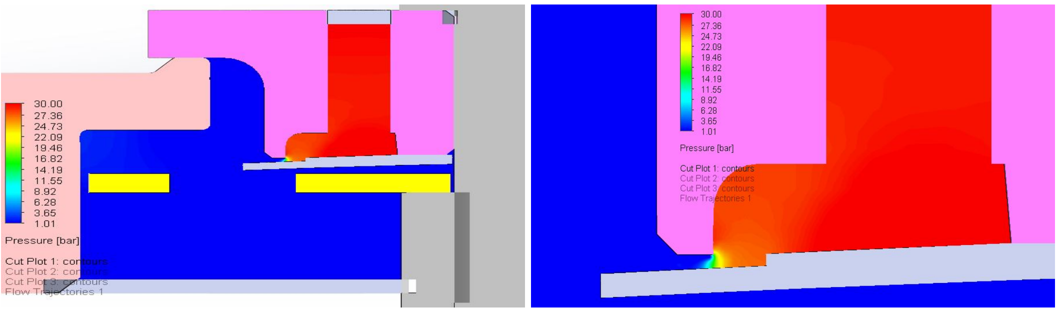

(a) (b)

Figure 5.6: Full assembly model 30 bar configuration,(a) carved region mid plane, (b) enlargement.

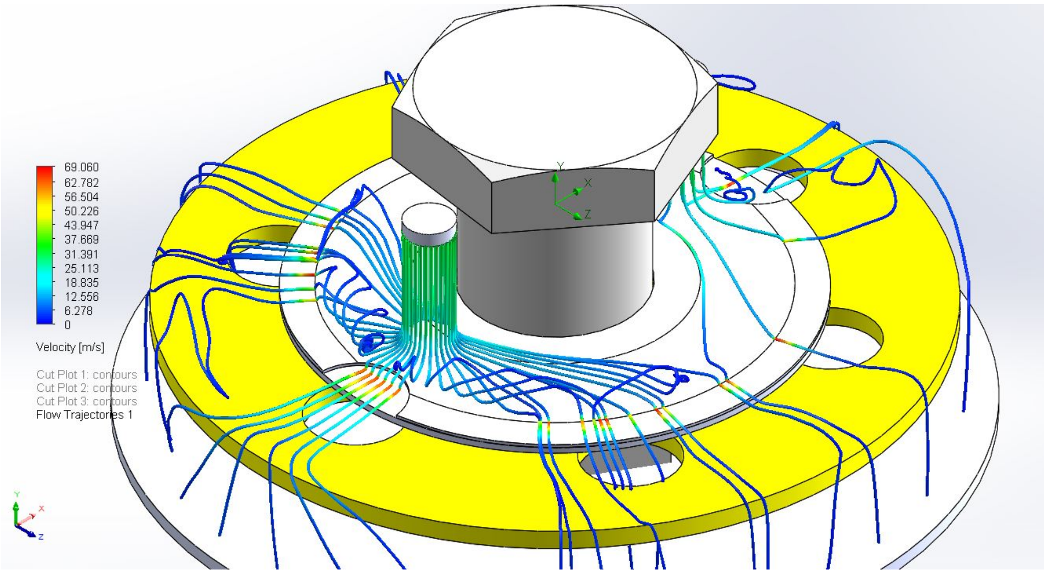

Figure 5.7: Flow trajectory speed color plot.

5.4 Symmetric model

After the recognition of the critical issues for the full assembly model, it is time to overcome them by using other methods for the geometry definition, because it is required to set up the CFD simulations. The main idea is to substitute the assembly with only one component that is representative of the total geometry. One component alone is not sufficient to completely define the geometry when it assumes the meaning of refining regions. Therefore one component will be representative of the total geometry and other ones will define the regions where the mesh must be refined. With the condensation of all the solid components in one element, is associated a simplification of the geometry. First simplification is the absence of gaps between components at the interface regions. This reduces the total quantity of cells as first result and also avoid to spend time in computing fluid behaviour in regions that are not of interest. The other simplification consists in the missing of that volumes where variables describing the fluid behaviour are considered constant. That regions are the cylindrical volumes that have been modeled as restrictor S3 and the surroundings around the valve where there is no flow. The simplifications already described are not sufficient to fulfill the mesh requirements in terms of maximum number of cells and level of refining in channels of interest. The two requirements are joined by using the symmetries of the valve. It is not completely axisymmetric but it is mirrored respect the frontal and the lateral plane. The study, therefore, can be limited to only $\frac{1}{4}$ of the model, giving the possibility to describe the metering region in more precise way.

5.4.1 Components

The geometry definition for the simulation is resumed by the building of a CAD model representative of all the details that are important to characterize the flow behaviour. The item modeling starts from the sketch of the restricted area where the fluid is throttled. The vertical deformation of the shims at the radius coincident with the metering edge is not equal along all the circumference, but it is higher far away carves. To equip the model with this feature costs in terms of effort, and it can be done directly by importing the deformed shape computed with the finite element structural analysis. As it has been made for the complete assembly model. One of the task of the symmetric model is to have a consistent geometry simplification. Therefore as distance between top and bottom surface of the metering region has been considered the average deformation along all the circle representing the metering edge. Another simplification is the missing representation of the zones where the flow behaviour is out of interest for the analysis. Like the volume inside restrictor S3 or the volume after the limiting disc. Like the case of complete assembly model, the regions where higher mesh refining is required are defined by using extra components with shape equal to the region of interest. Figure 5.8 shows the model in isometric view, where the control volume is underlined and the supplementary bodies are visible in red and yellow color. Then figures 5.9 and 5.10 are showing 2 section of interest for the model, respectively the carved one and the restricted one.

5.4.2 Boundary conditions

The boundary conditions set-up is performed in the same way of complete assembly model. In order to compute the volume flow rate that crosses the valve for a specified

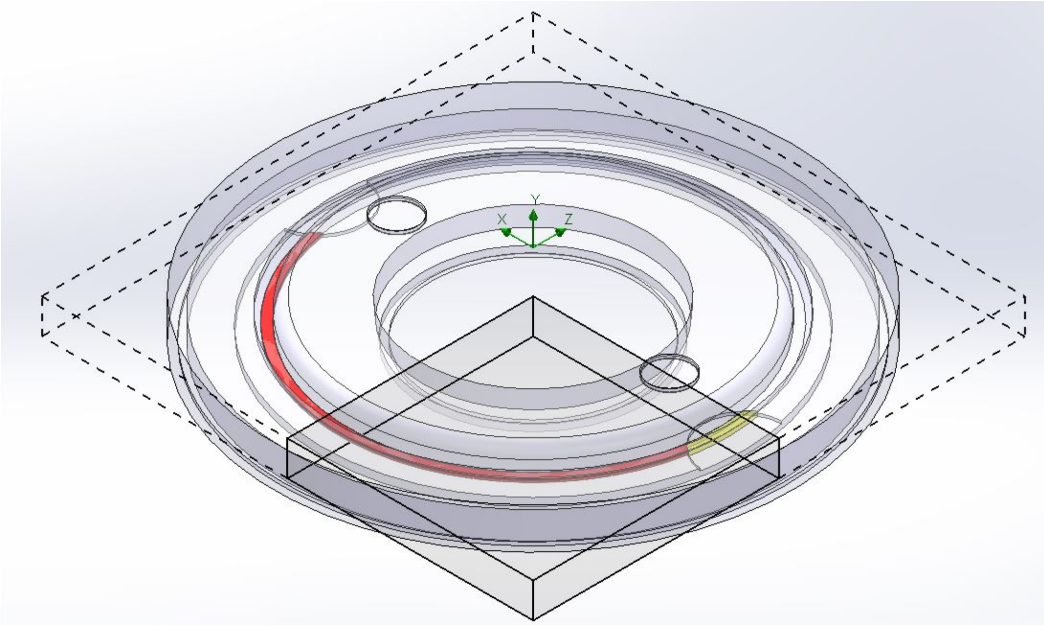

Figure 5.8: Symmetric model control volume.

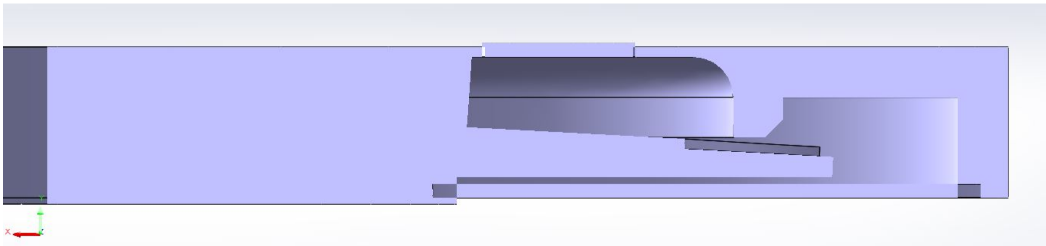

Figure 5.9: Carved region section view.

configuration, the respective pressure level is assigned to the internal surface of the intake lid, and environmental pressure level is assigned to the internal surface of the exhaust lid. Also for this model the volume flow rate that crosses the valve is set as surface goal for the intake chamber. Next step for the model characterization is the mesh generation.

5.4.3 Mesh

The mesh generation is always a crucial operation for the simulation purpose. In this model the mesh refinement is facilitated due to the subdivision of the computational domain in four symmetric parts, where only one is used for the computation. This ploy gives the possibility to refine better the zones of interest, as the metering volume and the carved zone on the top disc. In that case the maximum number of cells is used to discretize only a quarter of the valve. When using this method it is important

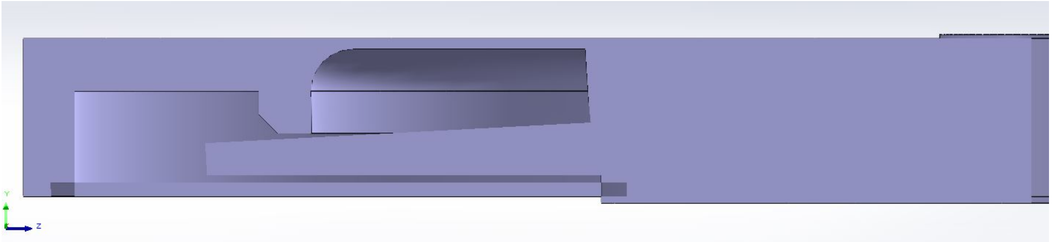

Figure 5.10: Restricted region section view.

to remember that the resultant volume flow rate must be multiplied by four, when it is required to obtain the total volume flow rate allowed by the VC. As already explained the regions where the oil is throttled are refined by the definition of a local mesh. It is characterized by a solid body that defines geometry and position, then disabled. The local mesh is completely defined by the selection of the refinement level. The refinement regions are shown in 5.8, where the body used to model the carved zone is colored in yellow. Instead the body used for the definition of the local mesh for the restricted part is the one colored in red. Using that geometry that does not include the restrictor S3, its influence is not taken into account. This choice has been made for two reasons, first to avoid the pressure drop due to the restrictor behaviour. It reduces the pressure in the annular volume that is supposed to be at 30 bar. Therefore it models in a more realistic way the phenomenon under investigation. Second reason is the reduction of the control volume dimensions, that simplify the mesh refinement process. Figure 5.11 and 5.12 show the mesh refinement in the regions of interest. In this case all the requirements have been satisfied, the total number of cells is around 2.4 millions and all the channels have been discretized using more than 10 cells for its smaller dimension.

5.4.4 results

The CFD simulation of the symmetric model has been performed without issues. Due to the the high level of discretization in the regions of interest, the results should be enough reliable. The pressure distribution on the top surface of the carved shim is almost constant and around 30 bar. As expected there is a reduction of the oil pressure far away from the intake hole. The pressure drop is exploited in all the restricted section. Due to the geometrical simplifications the valve model behaves symmetrically. The main result of the simulation is the volume flow rate that is throttled by the valve for a pressure drop of 30 bar. For a quarter of the model, the computed flow rate is equal to 1.535 l/min. To obtain the total flow rate it is sufficient to multiply this value by four, the result is 6.14 l/min. This value is not far away from the one obtained by using the full assembly model. The simplified and symmetric model is still not sufficient to study the minimum opening configurations, therefore a simpler model has been tested, it is described in the following paragraph.

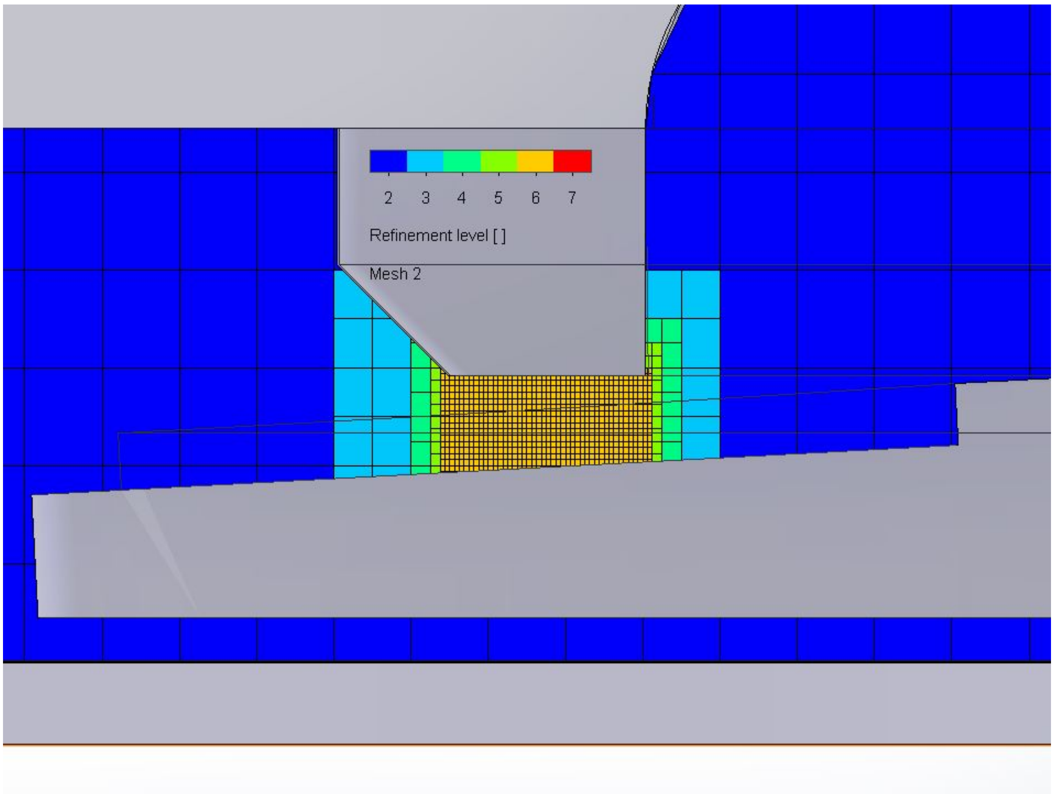

Figure 5.11: Mesh refinement in carved region.

5.5 Slice model

For the VC configurations of minimum opening was not possible to satisfy all the mesh requirements by using the full assembly model or the symmetric one. Therefore a more simplified model has been defined. Where instead of using the original CAD model of the valve, a new one has been modeled in simplified way. In the previous simulations, provided by complete geometry, has been detected that the flow lines in the metering region are almost parallel and oriented along the radial direction. It is clear that the only geometrical factor concurring in the simulation result is the distance between the top disc and the metering edge, and not the angular extension of the model. The slice model has been made in order to focus the research on the metering edge. Instead of studying the complete VC or a quarter of it, the simulation uses only a slice of the valve with fixed angular range. This method requires to create 2 models, one representative of the region where carves are present and the other one representative of the restricted section.Then the total volume flow rate that crosses the valve is obtained by the sum of all the contributions coming from the two models.

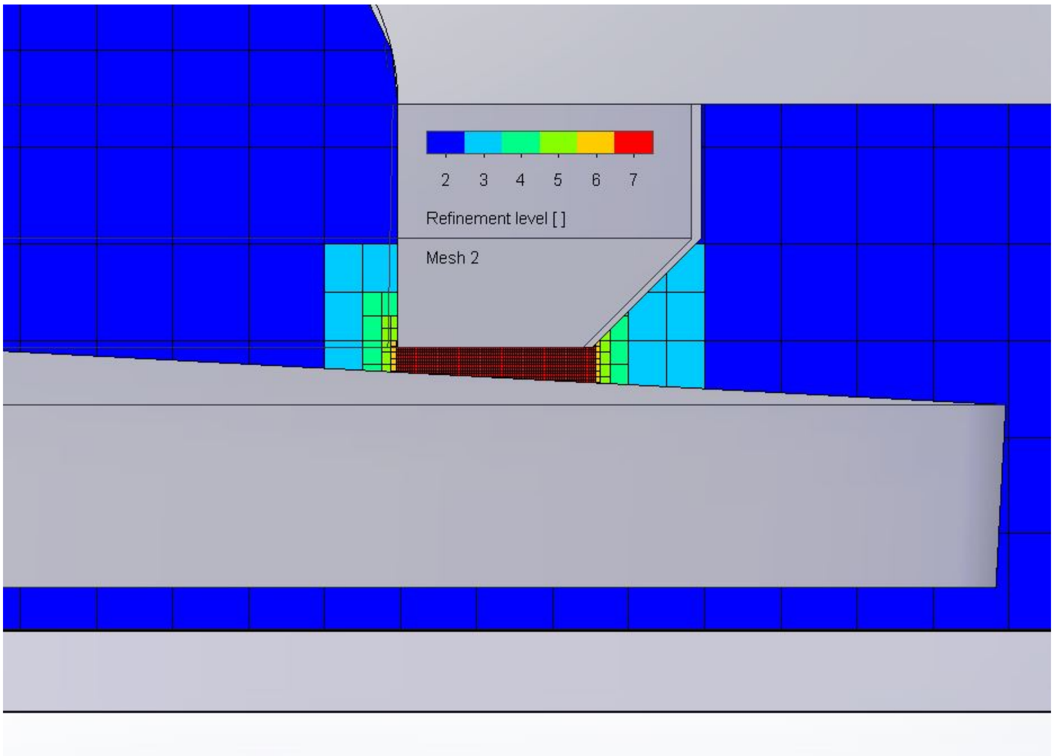

Figure 5.12: Mesh refinement in restricted zone.

5.5.1 Components

In this model the geometry is defined by two components. The top one reflects the shape of the valve body and the bottom one instead represents the deformed shim stack. The top component can be used for simulating all the opening configurations, instead the bottom component must be modeled in a number equal to the total quantity of configurations that are going to be tested. The bottom component has been modelled by using as reference the result of the FEM simulations. The profile of the deformed shape is not linear, but it has a quadratic shape, in similar way to beams subjected to a distributed load. For the objective of the simulation the profile shape of the component representative of the shim stack is not crucial. The most important geometrical feature is the distance between the metering edge and the carved shim. Therefore the profile of the bottom component has been modeled with a linear trend, connecting the point corresponding to the vertical displacement of the free edge and the one in correspondence to the clamped one. Then the sketch has been circularly extruded for a determined angle. In particular, for the testing of the restricted area it has been chosen 15 deg to reduce the computational domain dimensions, that helps having enough mesh refinement not exceeding the maximum number of cells allowed. The slice model for testing the carved zone extends for an angle of 30 deg, because, first it is required to cover the entire carved region, responsible of the throttling under minimum flow condition. Then the geometry is less critical, due to a higher gap dimension, that requires minor refinement level with respect to the restricted zone. The two models are shown in figure 5.13.

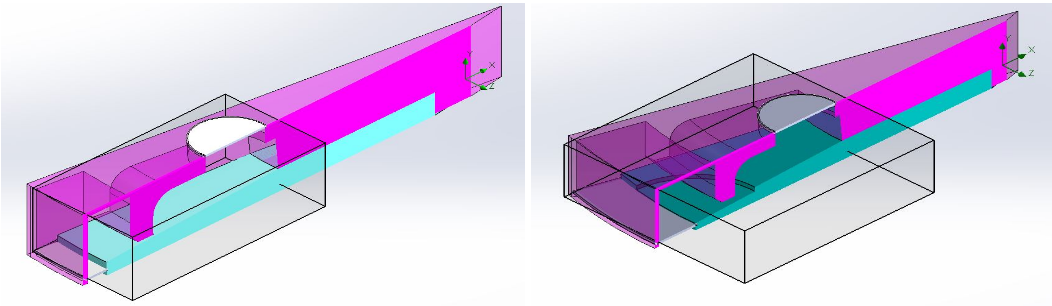

(a) (b)

Figure 5.13: Slice model ,(a) restricted region assembly, (b) carved region assembly.

5.5.2 Boundary conditions

In this kind of model several simplifications regarding the geometry have been assumed, but in a way that takes into account the most important features of the CV. The volume downstream the restricted area has been considered at environmental pressure, by setting this pressure level on the surfaces enclosing the volume. Instead for what concerns the intake, it has been made with an opening on the top component, then closed by a dedicated lid. On the internal surface of the intake lid the pressure has been set-up equal to the the value corresponding to the deformed shim associated. Next step before to launch the simulation is the mesh generation.

5.5.3 Mesh

The objective of this kind of model is to built an environment where the required mesh refinement does not causes issues due to an excessive number of cells. In order to test correctly the valve in the first opening configurations with the full assembly model are required more than twenty millions of cells. Using the slice model instead, only a portion of the valve is simulated, this implies a massive reduction of the total number of cells. In particular the total of fluid volume cells easily goes under the limit of three millions for all the configurations tested. In some cases, to respect the limit number of cells was necessary to set up a symmetry plane, dividing the slice in other two parts and consequently halving the fluid volume that is going to be discretized, but maintaining unchanged the main features responsible of the phenomenon characterization. Figure 5.14 shows a cut plot of the mesh in the zones of interest for both two the configurations, restricted region model on the left-hand side and carved region model on the right-hand side.

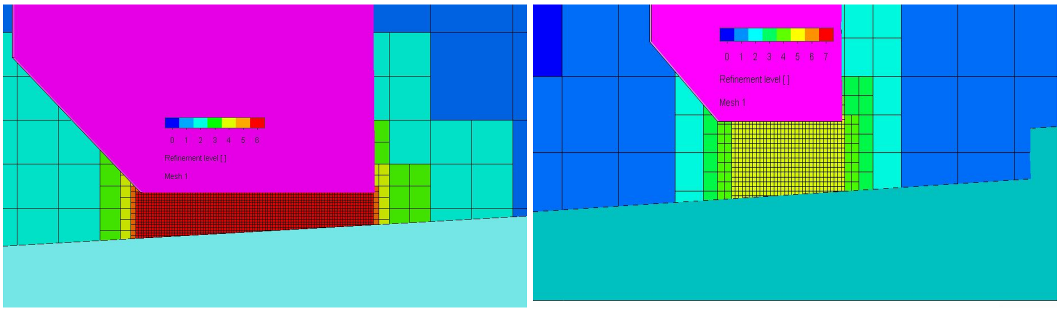

(a) (b)

Figure 5.14: Slice model mesh ,(a) restricted region model, (b) carved region model.

5.5.4 results

All the requirements in terms of mesh refinement and maximum number of cells have been satisfied. The model geometry has been simplified as much as possible, but maintaining the characteristics of interest for the study. The total flow rate that crosses the valve for the analyzed configuration is obtained with the sum of all the contributions. The carved model is wide 30 deg and there are two of them in the valve. The model that takes into account the restricted section is wide 15 deg therefore it contributes for 20 times. By the union of all the 22 slices the complete behaviour is obtained. The obtained volume flow rate is equal to 6.86 l/min.The contribution of the slice relative to the carved section is 1.16 l/min, instead the contribution relative to the restricted region slice is 0.227 l/min. Due to the easy way in which the slice model allows to study the valve, this kind of model has been used to extend the study to all the configurations of interest. Figure 5.15 shows the isosurfaces representation, it is used to visualize the spatial distribution of the pressure drop during the lamination process. The left hand-side picture shows the plot for the carved region, where it is putted in evidence the effect of the lateral walls, that are negatively influencing the simulation, the nature of the physical phenomenon is not modeled the best way. The same effect is visible in the right-hand side picture, where the same typology of plot is presented for the restricted region model. The presence of a virtual wall slowdown the fluid in the lateral wall boundary layer region, that is not coherent with the reality. The sharp metering edge causes an excessive pressure drop that in the worst case can lead to cavitation. Figure 5.16 shows the pressure distribution on the top surface of the carved shim. The pressure drop is concentrated in the strip close to the metering edge. This pressure distribution is in line with the initial hypothesis used to compute the shims deformation through the FEM analysis.

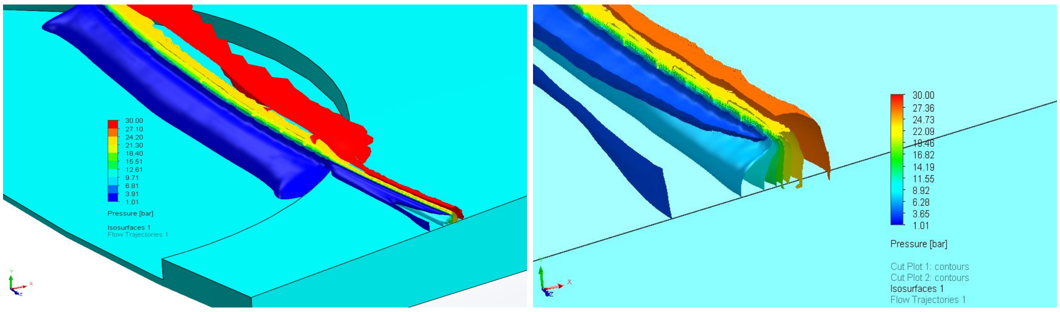

(a) (b)

Figure 5.15: Slice model 30 bar configuration iso surfaces,(a) carved region, (b) restricted region.

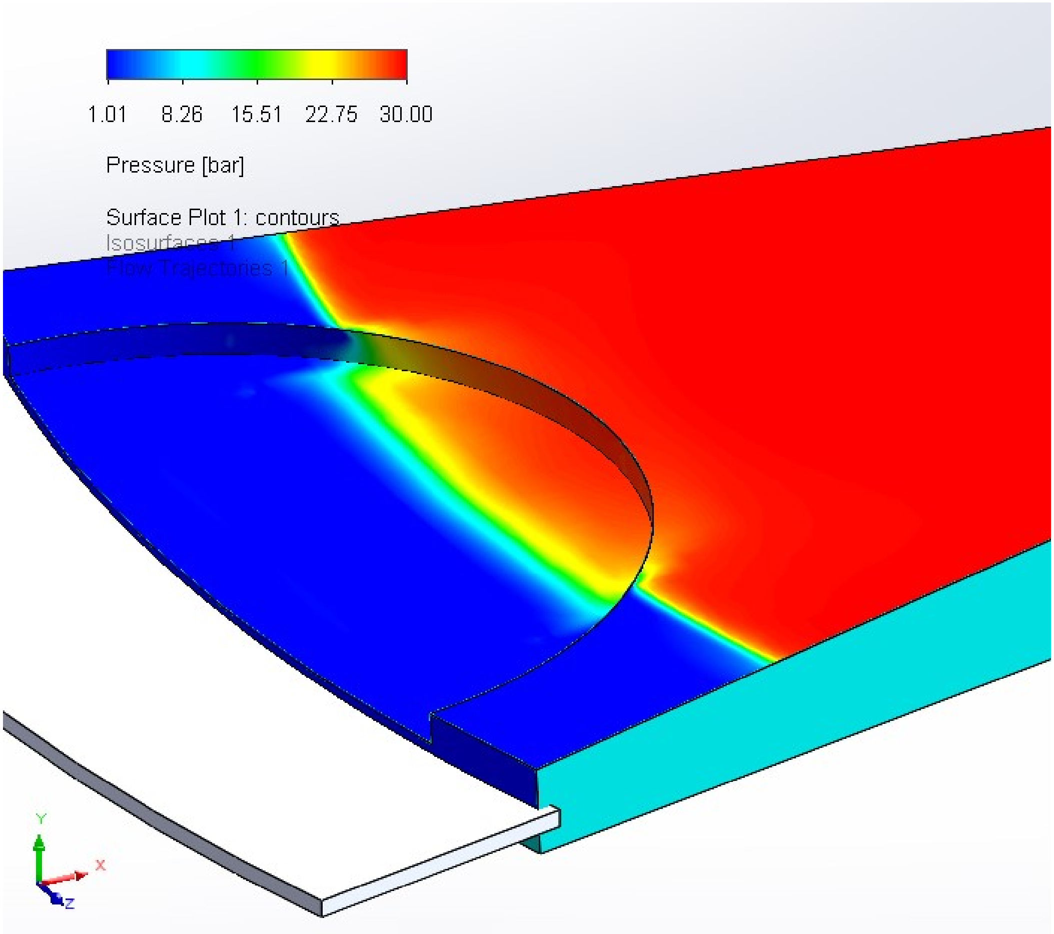

Figure 5.16: Slice model carved region pressure distribution on the top shim face.

5.6 Models comparison

Three CFD models of the the same system have been tested for the same configuration with the shim stack deformation at 30 bar. The full assembly is the most complete between the three models, but the issues relative to it do not permit the extension of the study to the other configurations of interest, with the available computational power. The symmetric model has overcome the problem associated to the S3 restrictor pressure drop and it allows a better discretization of the fluid volume by reducing the dimensions of the control volume. These simplifications are not still enough to extend the analysis to others configurations as the one of VC minimum opening. Finally, by the use of the slice model all the mesh requirements have been satisfied. By comparing the results obtained from the three CFD studies is clear that the massive geometry simplification, as in the case of the slice model, leads to an overestimation of the resultant volume flow rate. This can be due to the contribution of the restricted sections close to the top disc carves. The oil meets less resistance in the throttling through the carved region with respect to the restricted ones, therefore the overestimation of the volume flow rate can be traced to the sum of all the contributions that are considered equal, for the computation of flux where instead the real contribution of each slice can be different. However the difference between the results coming from the analysis of the first and last model tested is equal to 0.262 l/min, that corresponds to an overestimation of the 3.8%. Comparing the symmetric model with the full assembly one it is evident that the first one underestimates the volume flow rate. This can be the effect of the deformation averaging used for the simplified CAD model building. The underestimation performed by the symmetric model with respect to the full assembly one is of the 10.2%. The most reliable method between the two simplified ones with respect to the full assembly model is therefore the slice one. In any case only the experimental testing of the physical device could validate the results obtained by the full assembly model simulation. This can be caught as starting point for future investigations.

Chapter 6

Lumped parameter model

After the determination of the Q-p characteristic for the VC, it is the time for estimating the valve C_d. Its value can be obtained by reversing the formula that links pressure difference and volume flow rate for an orifice, because the only unknown parameter is the discharge coefficient itself. This coefficient depends on the Reynolds number at which the valve is working. Therefore it is not constant but it changes for each configuration that has been tested. The final output of this analysis is the influence of the CV on the damper behaviour. In order to achieve this result, a lumped parameters model has been made by using the Amesim software. Geometrical parameters were collected from the CAD model, fluid properties have been set equal to the ones used in the CFD simulations and instead of considering the C_d alone, it is considered its product with the flow area . The coil springs properties have been hypothesized due to lack of data. The lumped parameters model is a powerful tool, it gives the possibility to test several configurations of the system in a short time. It has been built reflecting the hydraulic schematics presented in the 3.4 paragraph, in the following ones the model is described more in detail.

6.1 Components

As explained in the previous chapters, the damper can be modeled by using three macro components, made by the assembly of sub components. First macro element is the differential linear actuator that mirrors the function of the tube piston assembly. Then the valves mounted on the piston, that together realize the VR, have been modeled with two parallel branches on which it is positioned, for each one, the sequence of restrictor and variable orifice, each one controlled by a coil spring. Last but not the least is the VC assembly, modeled with a pressure sensible variable orifice in parallel with a check valve for the back flow. Going more in depth, the variable orifices of the VR have been modeled by using the hydraulic components available in the software libraries. In figure 6.1 are shown the components used to model the VR in particular, the elements used for the variable orifice. Each one has been modeled with 3 sub-components, two of that coming from the hydraulic library and 1 from the mechanical components one. With respect to the flow direction, first sub-component

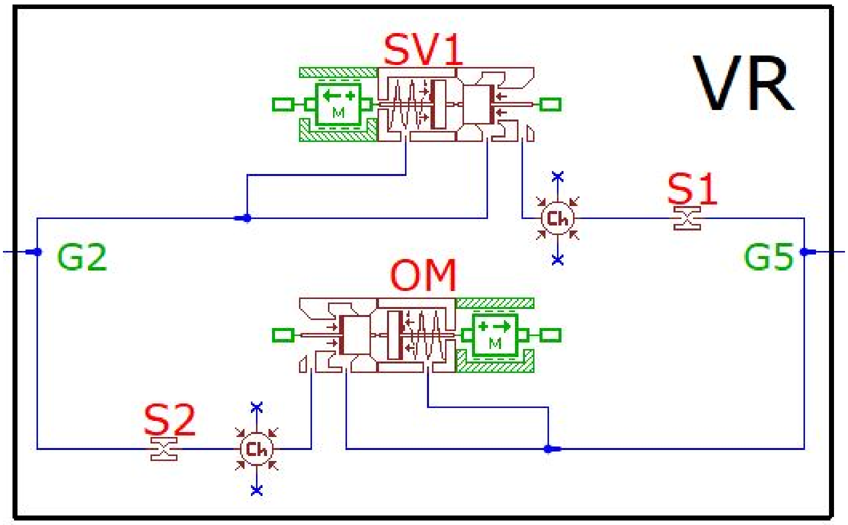

Figure 6.1: Rebound valve lumped parameters model.

used to model the variable restrictor is representing the cylindrical metering area that is varying as function of the poppet displacement due to the upstream pressure. It is followed by the element that takes into account the coil spring that holds in position the disc poppet and counteracts the force due to the upstream pressure that pushes toward the valve opening direction. The variable restrictor modelling is completed by a third element that includes mechanical data with a role in the valve working, like poppet weight and friction influence. That sequence of components is used for both the modeling of OM and SV1. The components are linked with pipe lines and junctions. Figure 6.2 shows the components used for modelling the VC. The NR is implemented using the same sequence used for SV1 previously described. SV3 instead has been modelled by using the variable orifice component already present in the hydraulic library. The opening of this component is controlled by a signal coming from a pressure sensor positioned upstream the variable orifice component. The pressure signal is converted in an opening signal through a look-up table that have been configured using all the data collected in the previous simulations. Figure 6.3 shows the sequence of components used to build the double effect actuator model. The components at the two boundaries take into account the surfaces of action of the piston. The components positioned in the middle instead are used to consider piston sealing and friction phenomenon to which the piston is subjected.

6.2 Discharge coefficient

One of the main objectives of this work consists in the computation of the C_d for the shim valve that is part of VC. The relation that links pressure drop and volume

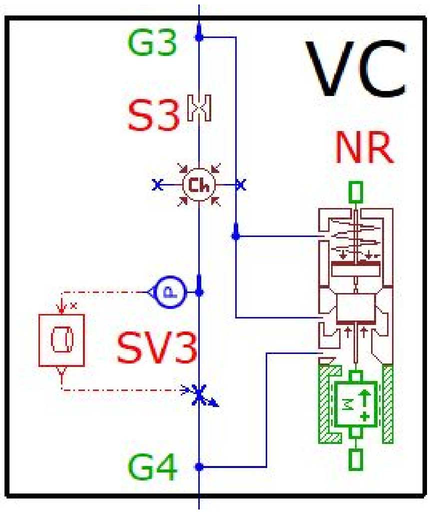

Figure 6.2: Compression valve lumped parameters model.

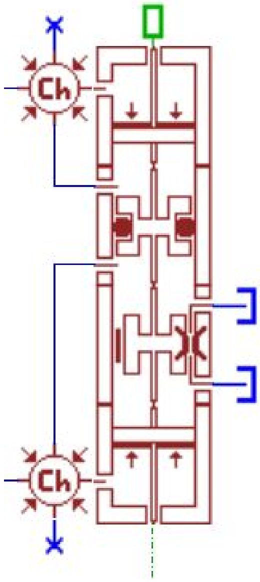

Figure 6.3: Double effect linear actuator lumped parameters model.

flow rate for an orifice includes the information about valve performance with respect to an ideal flow condition(discharge coefficient), the flow area dimension and fluid density. The pressure drop has been imposed, starting from that point the flow area has been computed through the use of FEM analysis,then the volume flow rate has been computed using CFD analysis, instead the oil density is a known data. Therefore by reversing the relation of interest it is possible to compute the discharge coefficient that characterizes the shim valve. The C_d has been computed as:

$$C_d = \frac{Q}{S\sqrt{\frac{2\Delta p}{\rho}}}.$$

Data and results of the computations are summarized in the table 6.1. For the first three opening configurations that have been tested, the resultant discharge coefficient is around a value of 0.47, it means that the *vena contracta* occupies less than the half of the space available for the flow passage. It can be due to the boundary layer, where the fluid is affected by the wall effect. In the last configuration tested, that corresponds to the maximum opening, the value of C_d increases till the value of 0.63. It means that the VC performs better in the conditions of maximum opening with respect to the others. Increasing the minimum distance between the surfaces that are defining the metering channel, the influence of the surfaces on the fluid flow is reduced. The software used for the lumped model development does not allow

Table 6.1: Numerical values used for the estimation of C_d.

Δp	Q	S	C_d
bar	l/min	mm^2	-
22	1.17	0.567	0.47
25	2.61	1.153	0.48
27	3.45	1.543	0.46
30	6.86	2.128	0.63

to use a variable discharge coefficient for the variable restrictor single component. Therefore it was decided to built the look-up table for the valve characterization using a single coefficient for each pressure drop configuration,that links the pressure drop to the opening configuration. This ploy allows to take into account the variation of C_d for each configuration tested. In order to use correctly this modelling strategy it is required to define the equivalent orifice diameter. It is obtained by reversing the formula for the circle area computation, where the diameter takes the role of unknown and the effective flow surface area is replaced by its product with the respective discharge coefficient for each configuration. Then the look-up table for the control of the variable orifice has been built using as input the signal coming from the pressure sensor positioned upstream the variable orifice SV3, and as output the normalized opening coefficient, that is equal to the ratio between the current corrected flow area and the corrected maximum one. With the adjective "corrected" it is intended the product of flow area and relative discharge coefficient. Using this ploy of including the C_d effect in the definition of the look-up table it is required to set it equal to 1 in the configuration of the variable orifice lumped parameter. The numerical values used for the look-up table are summarized in table 6.2.

Table 6.2: Numerical values used for the valve characterization.

Δp	$C_d * S$	S/S_{max}
bar	mm^2	-
22	0.267	0.199
25	0.558	0.416
27	0.712	0.531
30	1.342	1

6.3 Damper behaviour

The complete damper model have been tested in the Amesim environment. It is made by the union of the three sub-models previously described, figure 6.4 shows how they are connected. The input for the simulation of the damper behaviour consists in the application of an ideal speed source to the port that corresponds to its top ring, the other one is fixed. The trend of the speed source is sinusoidal with a frequency equal to 1 Hz, an amplitude of 0.3 m/s and a phase equal to π. The simulation time is equal to 1 s, therefore the test runs for one complete cycle of the damper, respectively compression phase followed by the rebound one. The damper behaviour is obtained by plotting the braking force as function of the rings relative speed. Furthermore the software permits to plot each physical quantity of interest, in order to better understand what happens inside each component.

Figure 6.5 shows the plot of damper braking force in function of rings relative speed, the curve is not symmetric with respect to the axis origin. For both the quadrants the curve can be identified with two trends, that are divided by a sharp knee. Starting from the origin the force developed by the damper increases linearly with respect to the rings relative speed. This behaviour is due to the progressive oil lamination controlled by the valves springs. After the knee the force has a parabolic trend, where it is evident a minor gradient respect to the linear part of the curve. In the non linear curve range the volume flow is almost turbulent and it is function of the several orifices that the oil meets during its movement from one actuator chamber to the other one. Until the volume that crosses the orifice does not overcome the saturation limit, the flow is controlled by the pressure that pushes the poppet against the coil spring, when the variable restrictor reaches its maximum opening condition it starts behaving as a fixed one. In the following sections the influence of springs characteristic and orifices dimensions are investigated.

6.4 Compression valve effects

Now it is time for explain the effects of the shim valve on the damper behaviour. Its main task is the dispose of the excessive volume flow rate when oil is passing from the compression chamber to the rebound one, where part of the volume it is occupied by the rod. The resistance to the flow that the shim valve exerts is

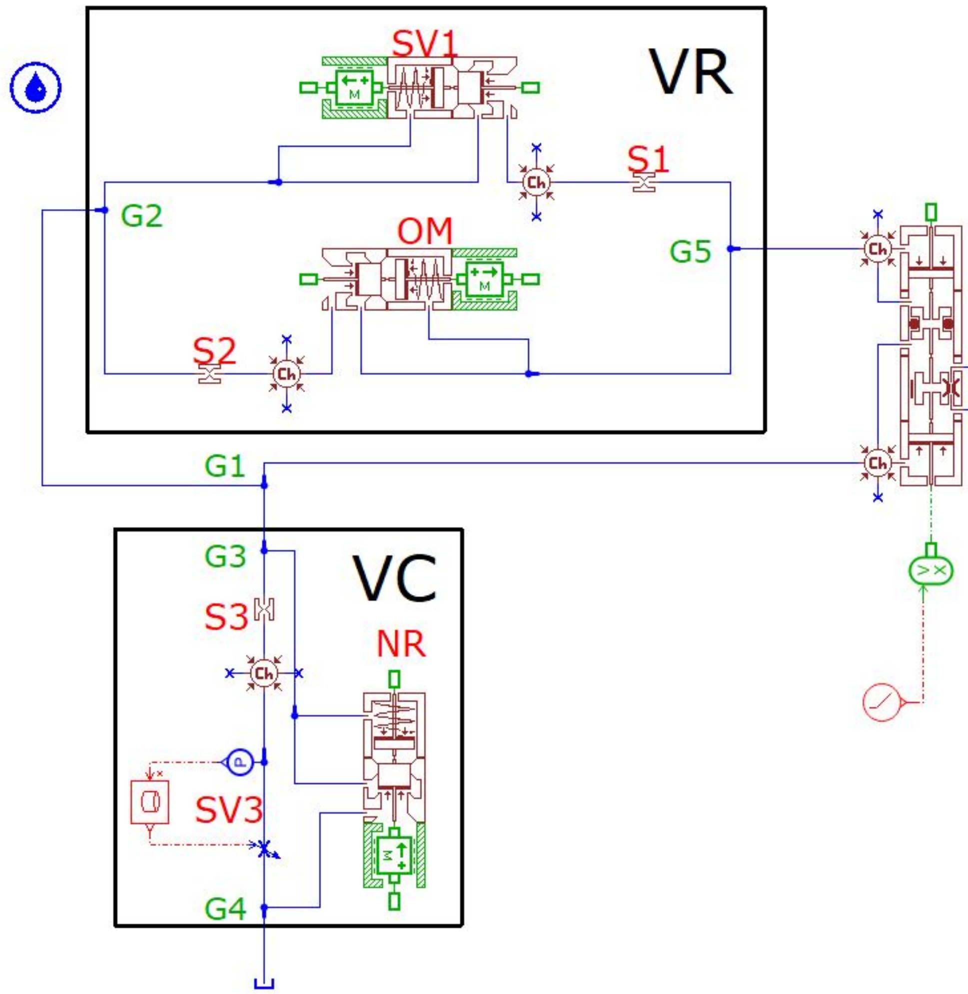

Figure 6.4: Amesim full model.

converted in a pressure boost inside the upstream chamber, then that pressure that acts on the piston active surface is transmitted as force by the rod. Therefore the VC characteristic directly influences the braking force developed by the damper in the compression phase. The VC is not alone in performing the compression tasks, great part of the lamination is performed by OM. The linear part of the damper characteristic is almost linear due to the effect of OM, that works in the same way of a pressure relief valve. The coil spring holds in closed position the guided disc poppet with its preload, as the oil pressure increases the poppet remains stationary until the opening force does not overcome the opening one. The opening force is given by the product of oil pressure and poppet active surface. The closing force instead is the sum of several contributions, as the viscous forces, the spring action and the friction

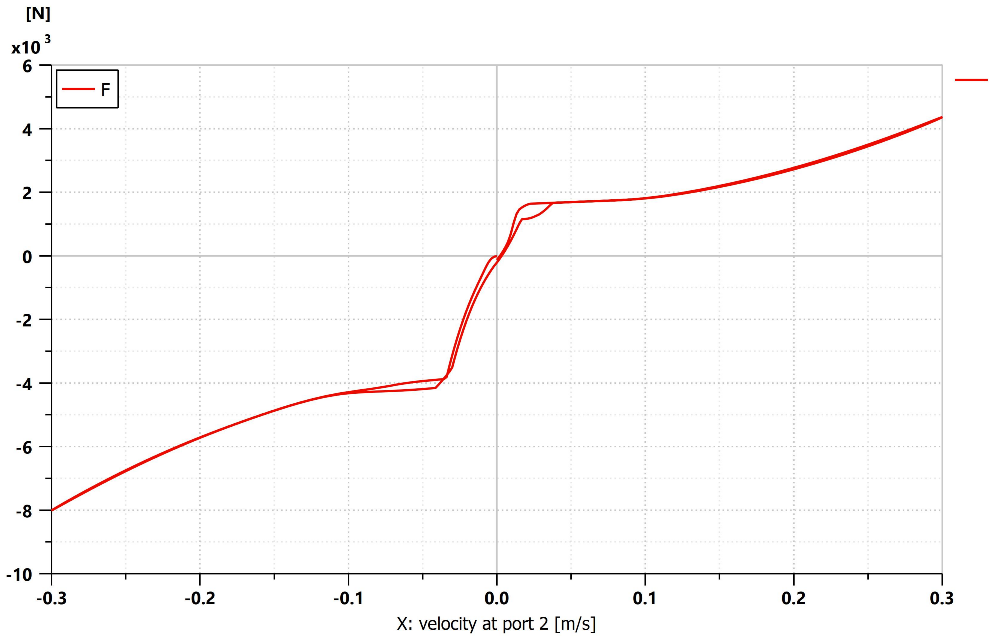

Figure 6.5: Force exchanged at the ring in function of the rings relative speed.

between sliding surfaces. The valve controls the flow until the poppet reaches the end stop, then it is obtained the maximum flow area. Therefore the metering device behaves like a fixed restrictor in saturation. In parallel to OM also SV3 laminates, but it starts opening with a small delay respect to OM. The equivalent stiffness and the preload of SV3 are higher than the ones of OM. If it were the opposite oil would flow first to the reservoir, leading to damper malfunctioning due to missing fluid inside the rebound chamber. Figure 6.6 shows the results obtained from the simulations of the damper behavior for three different configurations. In order to show the effect of the elastic members involved in the the compression phase, it has been chosen to plot the force at the ring position as function of time. The compression phase holds from 0 s to 0.5 s and it is followed by the rebound phase. In blue it is plotted the reference set-up, where it is implemented the shim valve characteristic obtained from the previous analysis. In red it is plotted the result of the configuration where the OM Spring preload have been doubled. The effect of this modification is the extension of the linear characteristic with a translation of the knee and a consequent increase of the maximum braking force reached in the compression phase. But this has an implication on the rebound phase, because increasing the flow resistance on OM can lead to an excessive flow to the reservoir, that means incomplete filling of the rebound chamber. The effect of the incomplete filling is the lack of force in the initial part of the rebound phase. In black it is plotted the result coming from the model configuration where, the computed shim valve characteristic has been substituted by a shifted one about 20 bar. It means that the opening characteristic starts increasing at a pressure of 32 bar and the maximum opening is reached at 50 bar. The effect

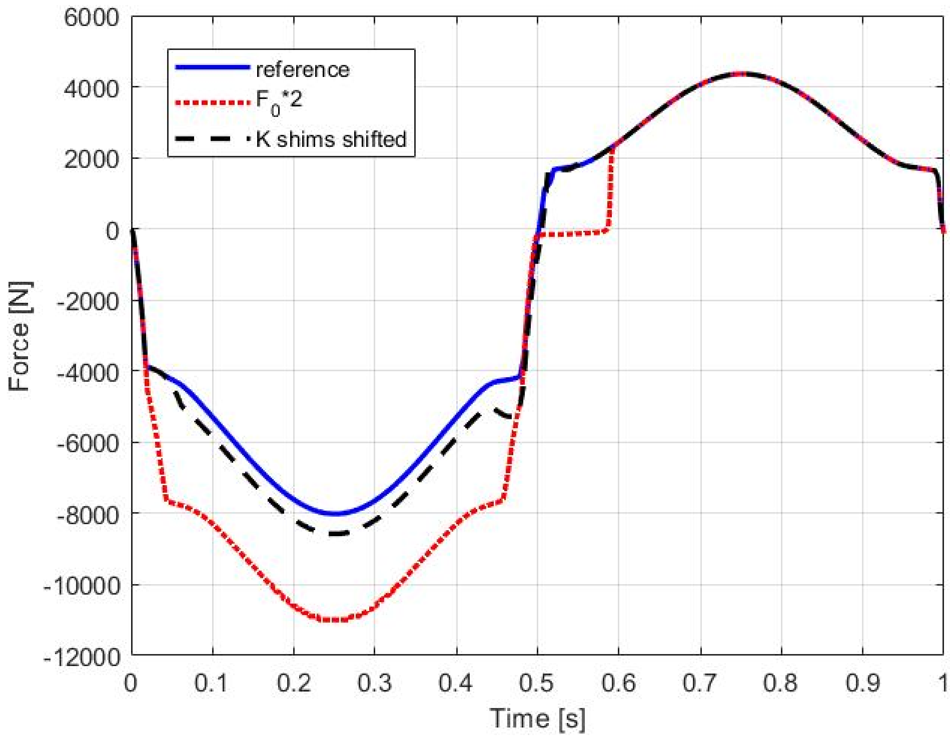

Figure 6.6: Comparison between reference behaviour and two modified set-ups.

is a shift of the force, increasing in absolute value, in the region of OM saturation. The damper behaviour in the compression phase depends also on the flow area of the fixed restrictor positioned upstream OM. Higher the surface lower the flow resistance. Figure 6.7 shows the comparison between the original configuration of S3 and one where the surface has been doubled. S3 in the reference configuration is made by 3 equal cylindrical holes with a diameter of 2.3 mm and a C_d equal to 0.7. The modified configuration instead has been set-up using six holes instead of three. The effect is clear, increasing the piston speed the forced volume flow rate increases too, due to the flow rate enforcement S2 behaves as compensator, therefore it imposes the pressure drop across it self. S2 holes are drilled on the piston, connecting one chamber to the other one. So the pressure drop across S2 multiplied for the piston active surface is equal to the force exchanged by the rod. The shape of the curve describing the pressure drop in function of the volume flow rate across S2 is equal to the F vs v characteristics but scaled by some proportional factors.

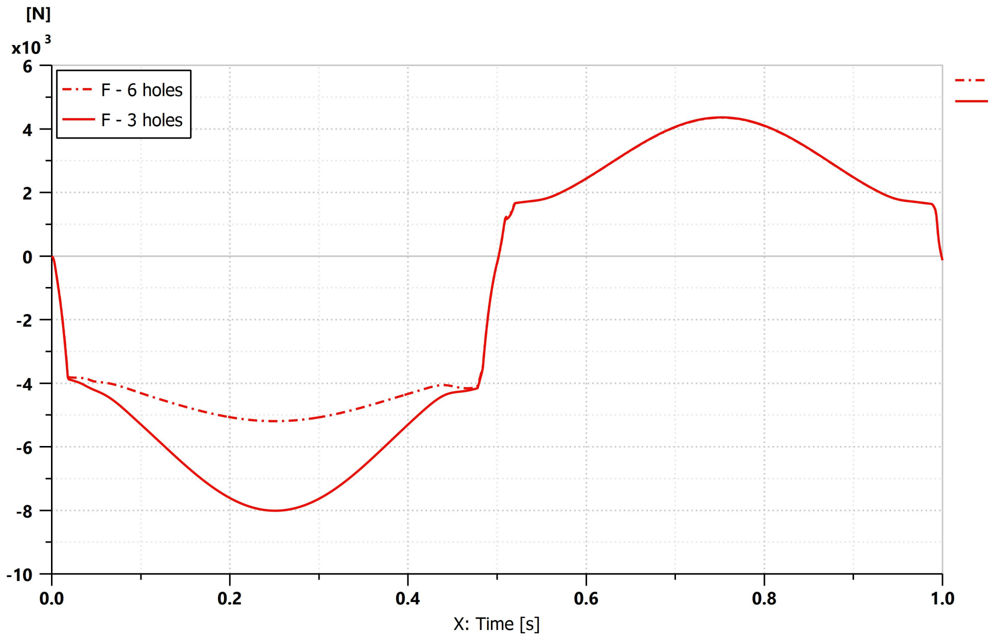

Figure 6.7: Comparison between original S2 flow area and doubled.

6.5 Rebound valve effect

The great part of this work is devoted to the VC, but also the VR plays an important role in the damper working. It is in charge of managing the rebound phase, when the rod moves in the outward direction. This phase is completely controlled by the characteristic of the spring mounted in SV1 and by the flow area of S1. The variable restrictor effect is predominant until it arrives to the saturation, for speeds higher than 0.02 m/s instead the predominant phenomenon in the damper behaviour is the saturation of S1. Figure 6.8 shows the comparison between three different configurations of the rebound valve. In blue it is plotted the reference configuration. The first modification that has been tested is the stiffness doubling for the spring included in SV1. Maintaining unchanged the spring preload displacement also the preload force is doubled. The effect is an extension of the linear characteristic range, due to the higher spring stiffness it is required a higher fluid pressure to saturate SV1 with respect to the reference case. The results of the other modified model are plotted in black dashed line, the modification consists in the reduction of the S1 flow area. The reference specifications of S1 are equal to the ones of S2 that have been described previously. In the modified set-up, instead of using three holes have been used two. The reduction of the total flow area implies an increase of the flow resistance that entails in an increase of force exchanged by the rod.

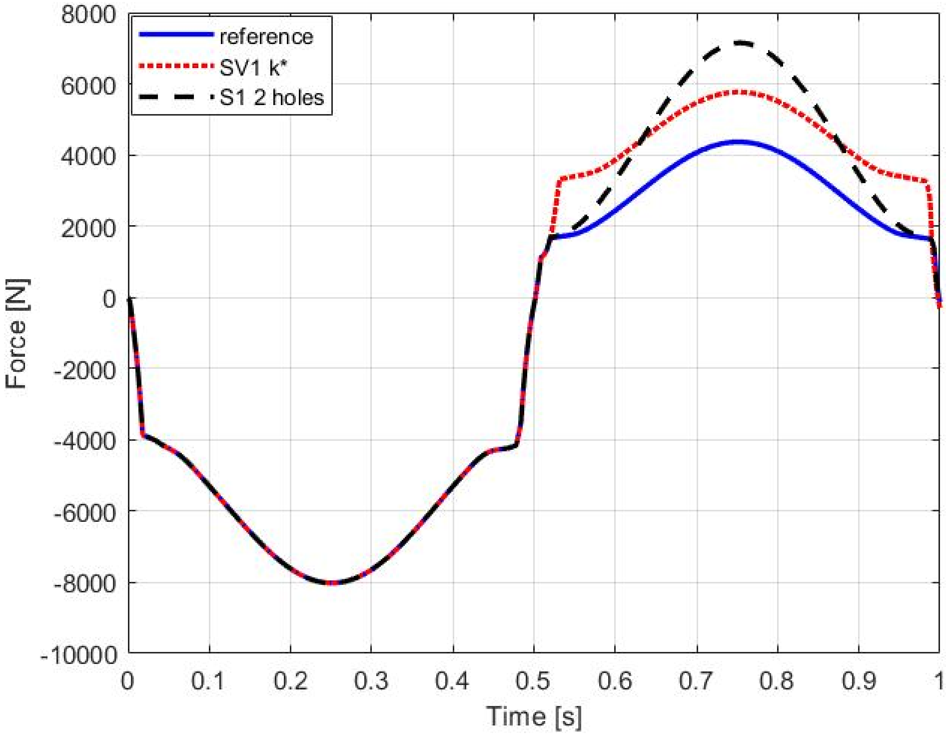

Figure 6.8: Comparison between 3 different configurations of VR.

Part III

Results and conclusions

Chapter 7

Results

7.1 FEM analysis results

In this section are presented the results obtained from the FEM analysis used to characterize the shim stack bending characteristic. The results are presented by the use of pictures; by means of colored plot, the qualitative aspects relative to the phenomenon under investigation are shown. Quantitative results are summarized by tables.

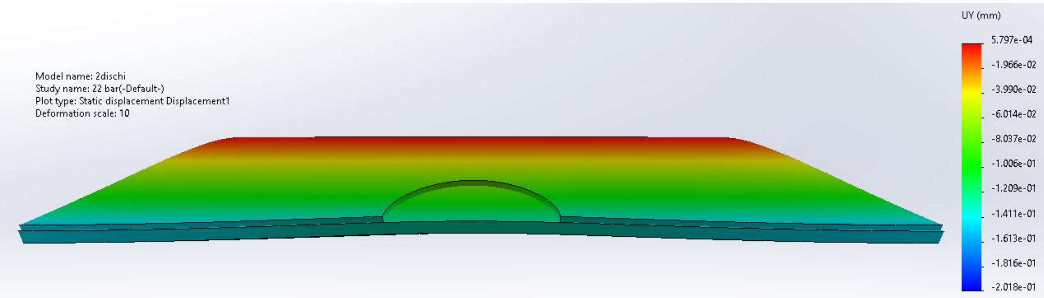

Figure 7.1: Deformation in the vertical dimension for a load of 22 bar.

Table 7.1: FEM analysis numerical results.

Load	Average deformation in correspondence of the metering edge	maximum stress
bar	mm	MPa
22	-1.013e-01	1,000
25	-1.151e-01	1,137
27	-1.243e-01	1,228
30	-1.382e-01	1,357

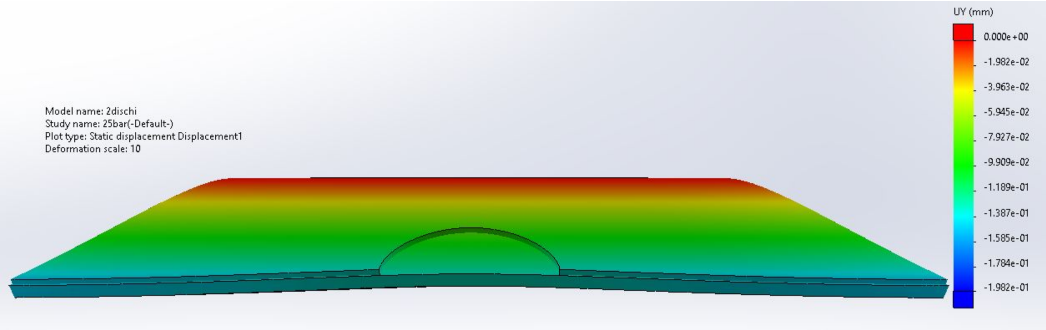

Figure 7.2: Deformation in the vertical dimension for a load of 25 bar.

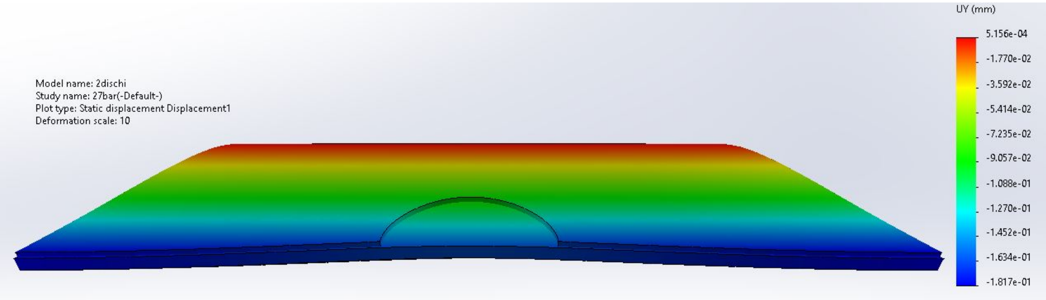

Figure 7.3: Deformation in the vertical dimension for a load of 27 bar.

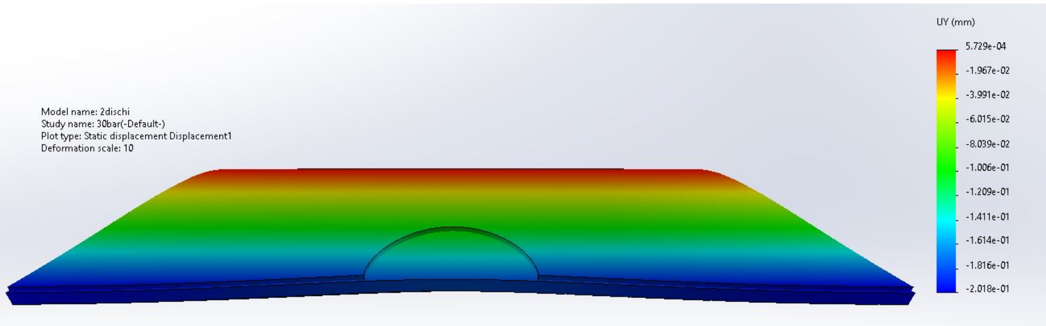

Figure 7.4: Deformation in the vertical dimension for a load of 30 bar.

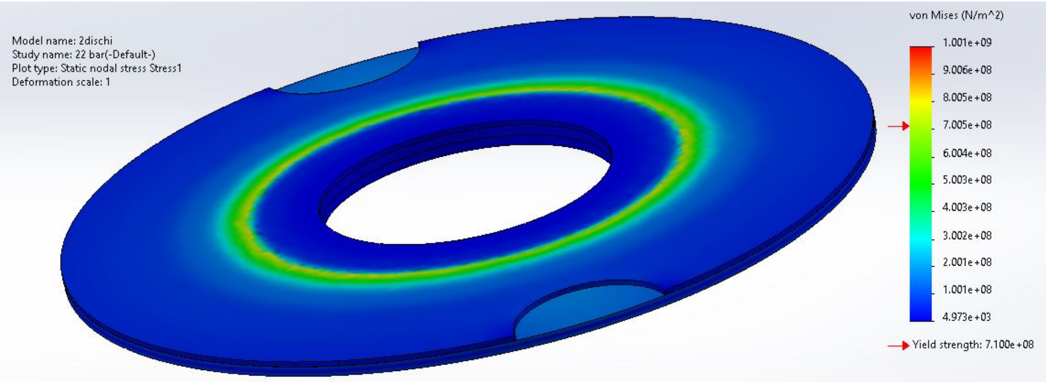

Figure 7.5: Von Mises averaged stress for a load of 22 bar.

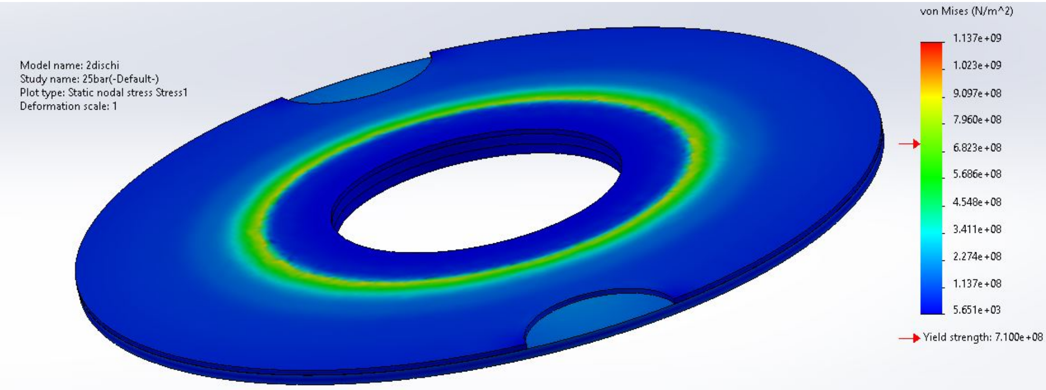

Figure 7.6: Von Mises averaged stress for a load of 25 bar.

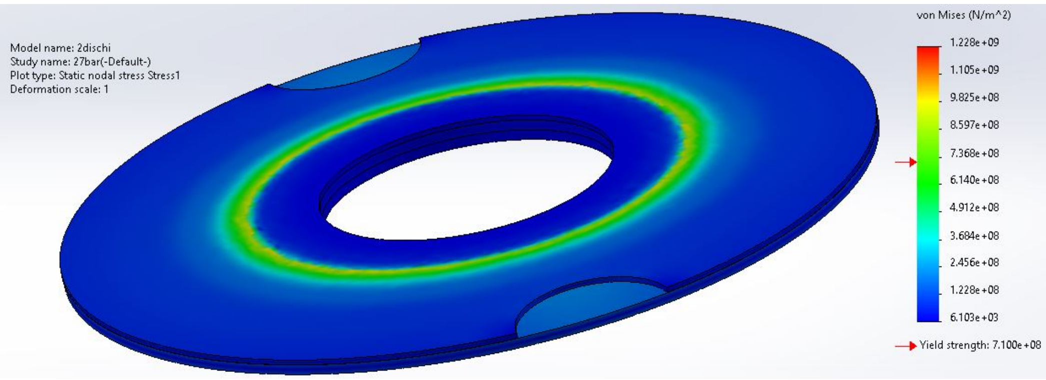

Figure 7.7: Von Mises averaged stress for a load of 27 bar.

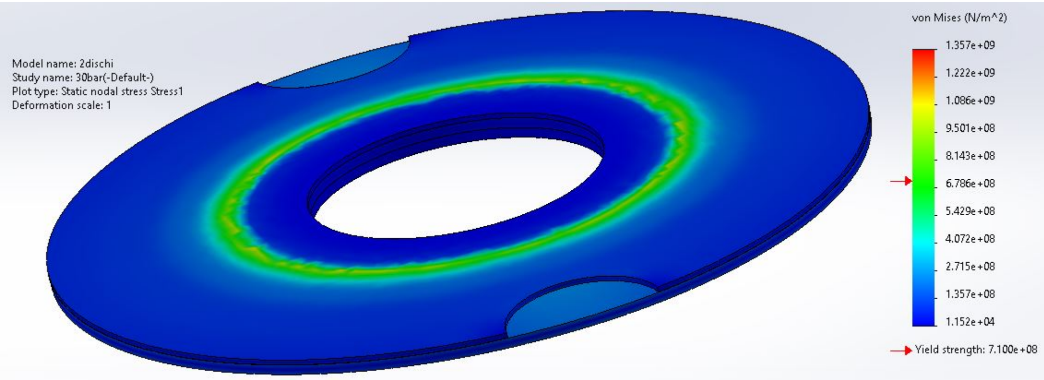

Figure 7.8: Von Mises averaged stress for a load of 30 bar.

7.2 CFD analysis results

The CFD analysis was the one that requires the greater effort. The results relative to the full assembly model and to the symmetric one have already been presented in the relative sections of this text. By the use of this two models only the 30 bar configuration has been tested, because it is the less critical one, allowing to run the simulation without issues relative to the mesh creation. Last model that has been tested is the slice one. It has been used to test the four load cases chosen. Now the results of those simulations follow. They are presented by the use of color plots. The main information of interest are the pressure distribution and the fluid speed.

Table 7.2: CFD analysis numerical results.

Load	restricted region volume flow rate	carved region volume flow rate	total volume flow rate
bar	l/min	l/min	l/min
22	0.003	0.579	1.218
25	0.056	0.741	2.606
27	0.086	0.876	3.467
30	0.227	1.162	6.862

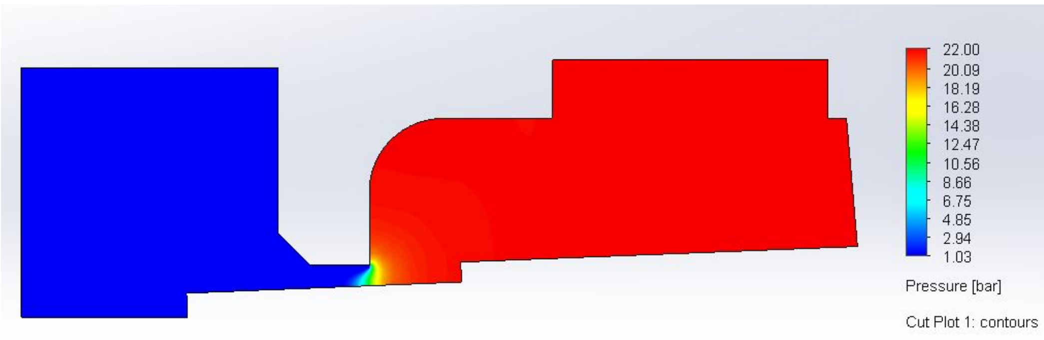

Figure 7.9: Mid-plane pressure distribution at 22 bar load, carved region.

7.3 Lumped parameter study results

Last model that has been presented is the lumped parameter one. The most interesting result is the force exchanged by the rod as function of its speed, that result has already been presented in the section dedicated to the lumped parameter model. Others interesting results obtainable with this model are the flow characteristics of the damper valves. They are obtained by plotting the allowed flow rate as function of the upstream pressure. The plots of interest are now presented. Figure 7.19 shows the damper hydraulic behaviour during the compression phase. The plots refer to the

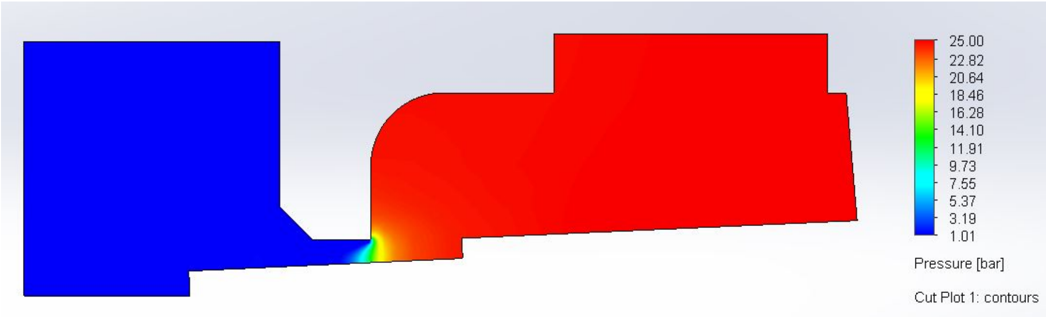

Figure 7.10: Mid-plane pressure distribution at 25 bar load, carved region.

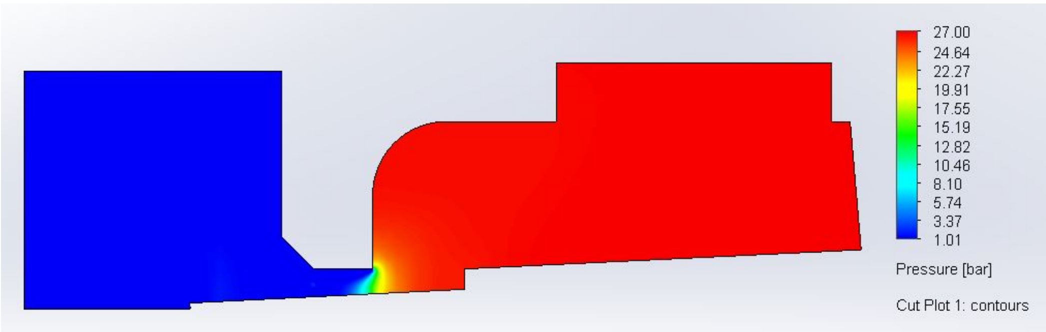

Figure 7.11: Mid-plane pressure distribution at 27 bar load, carved region.

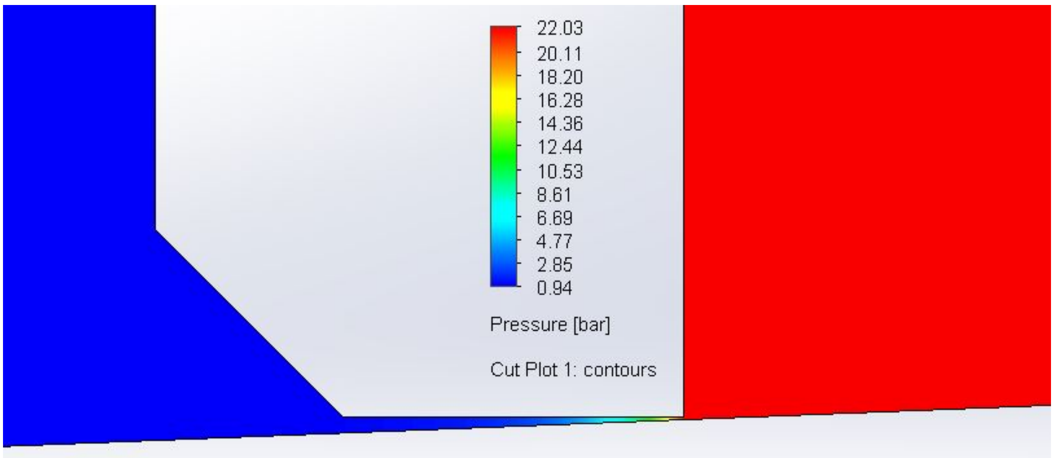

Figure 7.12: Mid-plane pressure distribution at 22 bar load, restricted region.

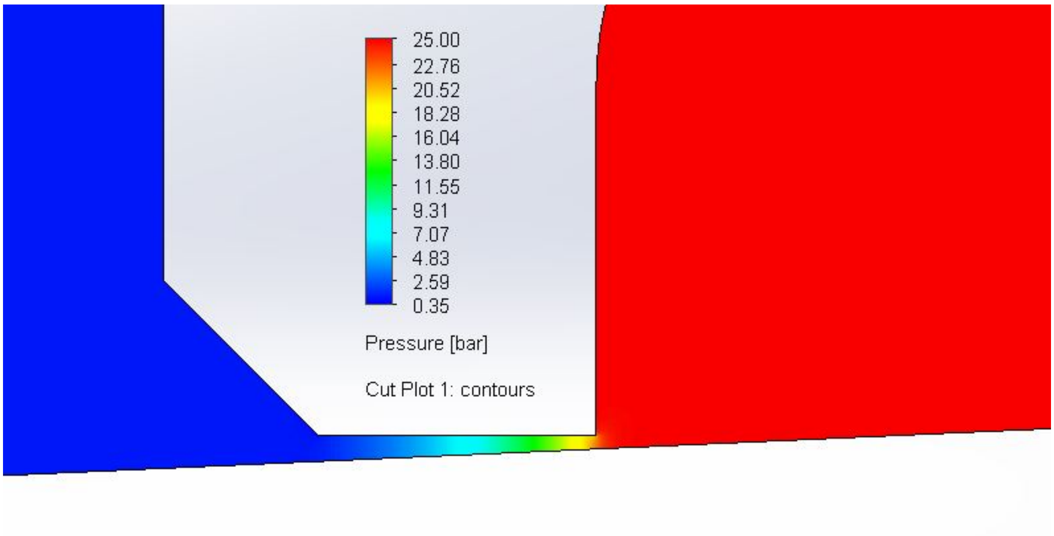

Figure 7.13: Mid-plane pressure distribution at 25 bar load, restricted region.

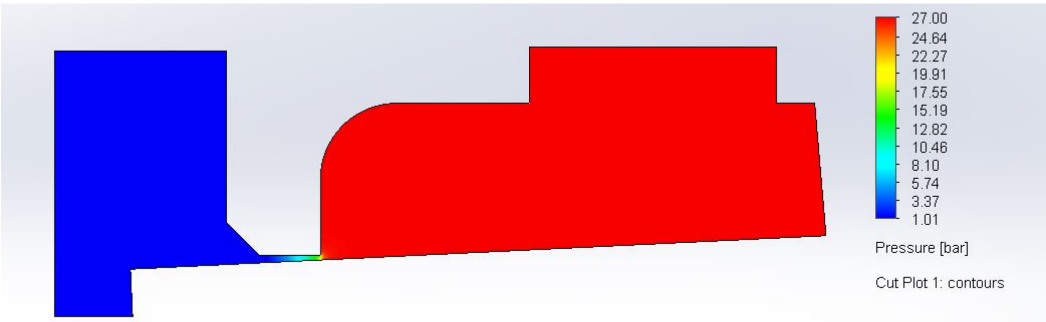

Figure 7.14: Mid-plane pressure distribution at 27 bar load, restricted region.

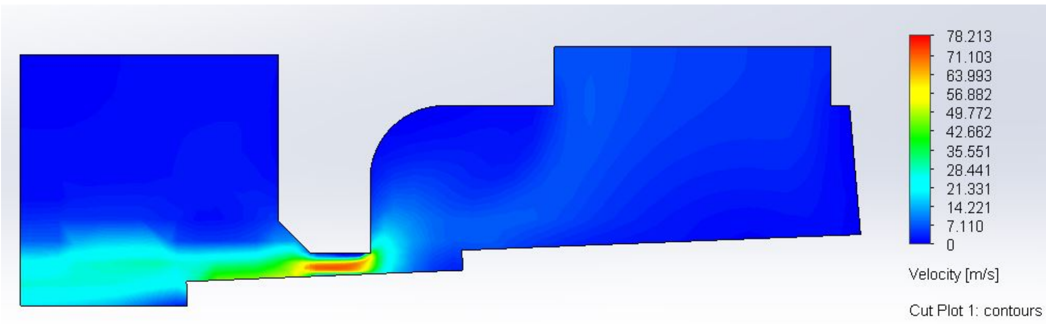

Figure 7.15: Mid-plane fluid speed distribution at 22 bar load, carved region.

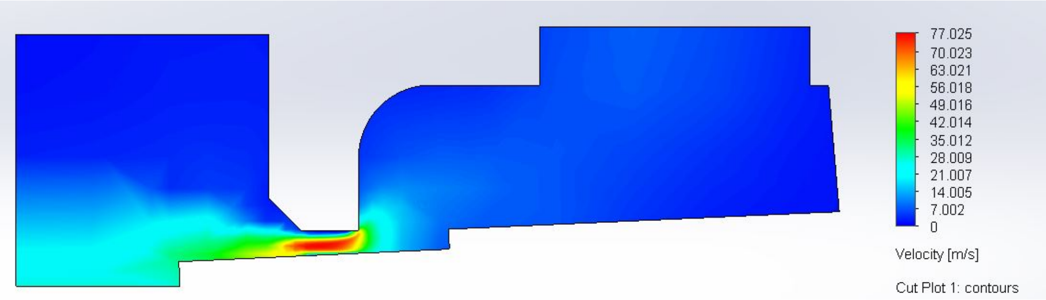

Figure 7.16: Mid-plane fluid speed distribution at 25 bar load, carved region.

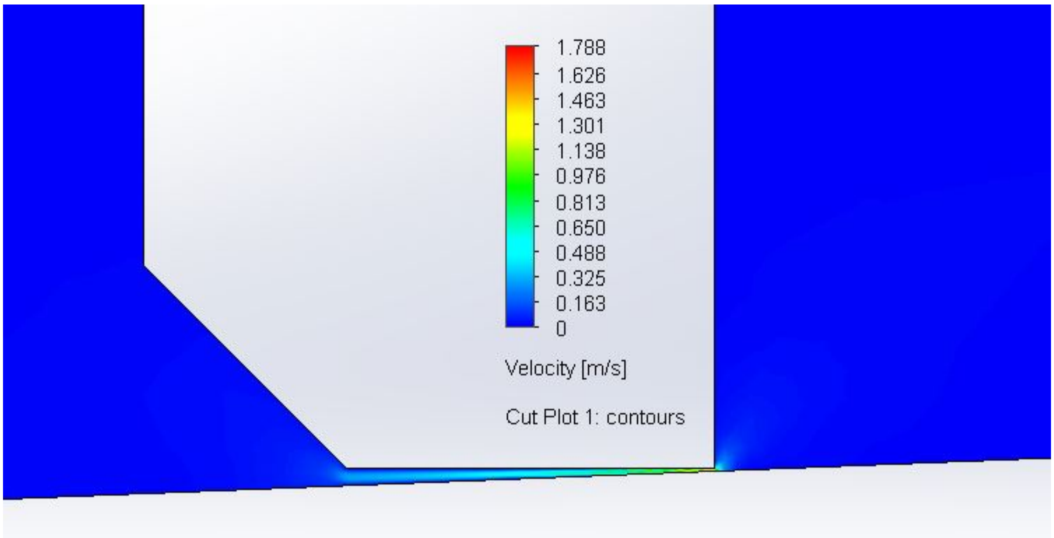

Figure 7.17: Mid-plane fluid speed distribution at 22 bar load, restricted region.

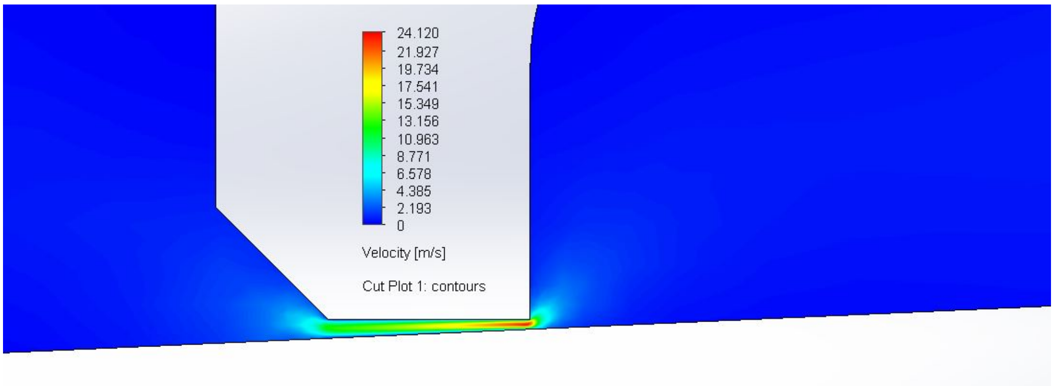

Figure 7.18: Mid-plane fluid speed distribution at 25 bar load, restricted region.

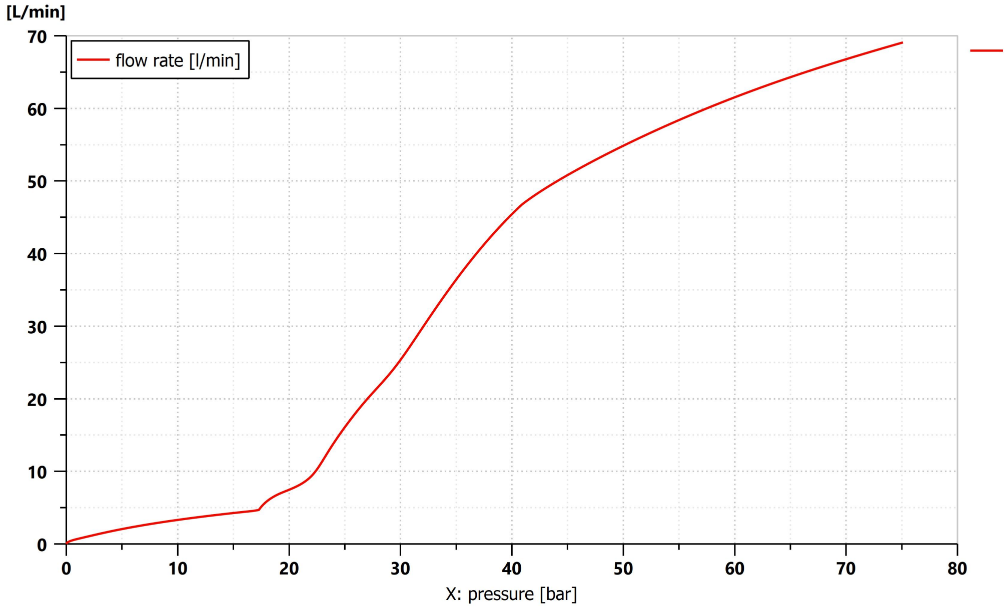

Figure 7.19: Q-p characteristic in compression.

flow rate that exits from the compression chamber as function of the pressure level inside it. It is possible to divide the behaviour in two part, first one is almost linear and it is due to the OM effect. After that the behaviour reflects the saturation of the orifices involved in the compression phase. Figure 7.20 shows the volume flow rate exiting from the rebound chamber as function of the pressure level inside it. Again it is clear the effect of the concentrated resistances, that the fluid flow encounters during its path from the rebound chamber toward the compression one. In the small extension speed range the characteristics are determined by SV1 that is regulating. When it saturates the compensation task is exploited by the fixed restrictor S1. Last result that is presented is the shim valve hydraulic behaviour, shown in figure 7.21. For pressures lower than 20 bar the valve is closed, but it allows the flow passage, this is due to the carves on the top shim. Then at the pressure of 22 bar the valve starts regulating until its saturation. It happens overcoming 30 bar, after this point the valve behaves like a fixed restrictor.

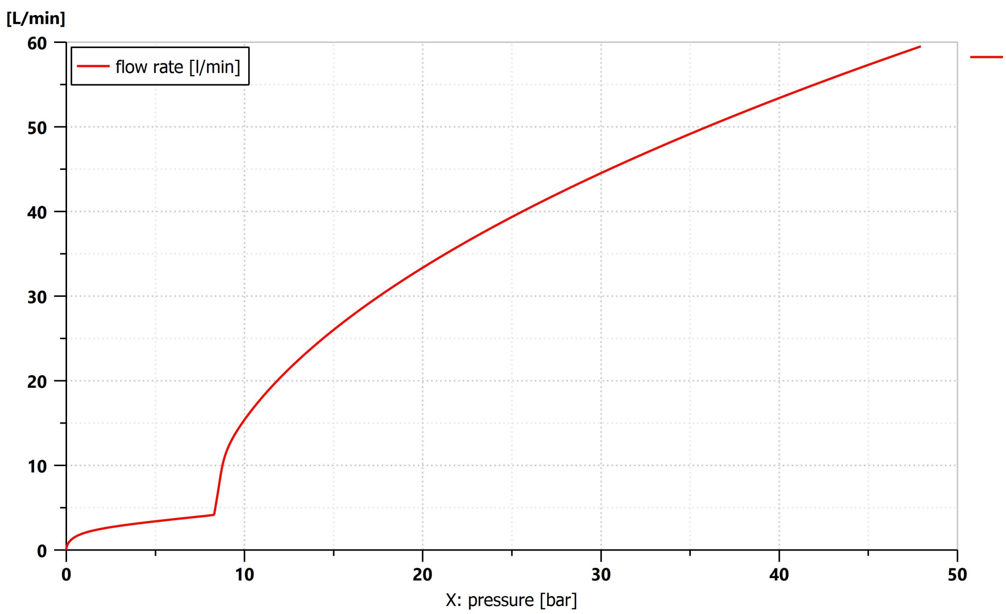

Figure 7.20: Q-p characteristic in rebound.

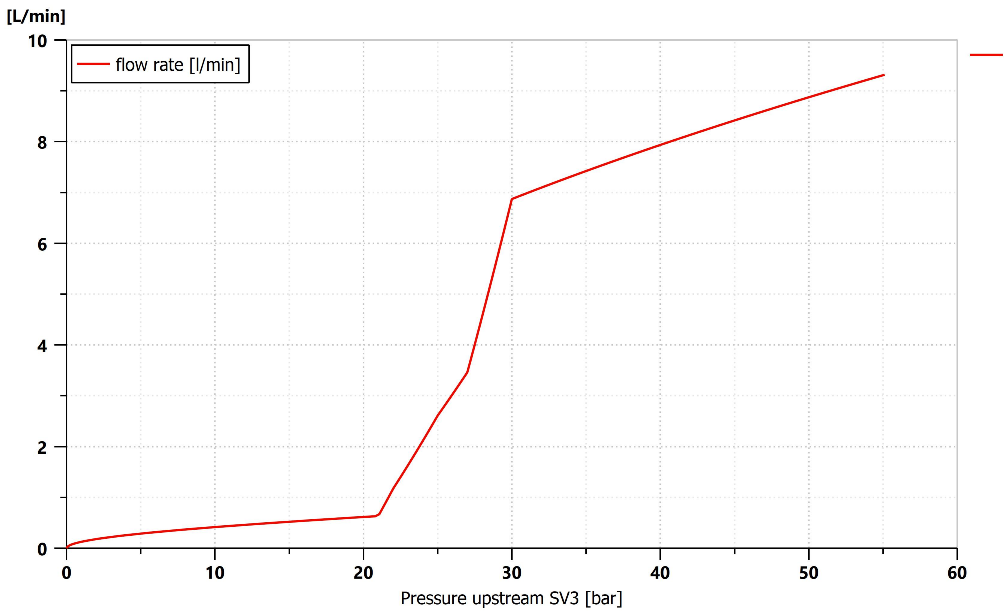

Figure 7.21: shim valve Q-p characteristic.

Chapter 8

Conclusions

Starting from the CAD model of a hydraulic damper other three models have been realized. First the FEM one, in order to characterize the elastic behaviour of the shims used in the VC. Then the CFD model has been realized in 3 versions with progressively reduced geometrical complexity. After that the third model has been set-up, where each component of the damper was included with respect to its function. Almost all the geometrical data were available in the CAD model, but the springs stiffness were unknown. For the coil ones it was hypothesized, instead for the shims it was estimated numerically. Also the hydraulic characteristics of the shim valve has been estimated numerically. The interest of producing a methodology for the hydraulic characterization of a shim valve has been satisfied. Then the effects of the shim valve and of the others components on the damper behaviour have been investigated. Several challenges have been overcome during the development of this work. The hardest one was to deal with limited computational power resources. It was useful to understand better how to exploit as much as possible the available resources. The accuracy of the results is limited by the approximations that have been made and by the software used. However this work can be a starting point for future analysis about hydraulic dampers equipped by shim valves.

Appendix A

How to import deformed CAD configuration resultant from FEM simulation.

This appendix wants to show the procedure that has been used for the realization of the CFD full assembly model, where the undeformed configuration of the shim stack has been substituted by its resultant displaced configuration, due to the pressure load action. The work has been performed by the use of the solidworks software for both the CAD modeling aspects and the numerical simulation. In the software is already implemented the option for importing the deformed body. It is sufficient to right-click on the *results* item of the project tree and choose the option $CreateBodyfromDeformedShape$ as shown in figure A.1. After that it is required to choose between the available options for the importation. As shown in figure A.2 it is possible to import directly the items in the solid configuration or instead in the surface one. It is also possible to import the components in the tessellated configuration, where the information about the mesh used for the simulation are included, but in this case it is not useful for that work objective. In this case is not convenient to import directly the solid body because at the interface between the two shims, their surfaces are not completely in contact as can be seen in figure A.3, this can be an issue for the following CFD simulation. The model must be leakproof, if there is an empty space between the solid bodies it can be recognized by the software as opening. To create lids for closing these openings is not easy due to the particular geometry. This issue can be overcome by the importing of surfaces instead of solid bodies. Then the surfaces representing the deformed body needs to be converted into solid bodies to be used in the CFD simulation. This operation can be performed using the surface tool $deleteface$ as shown in figure A.4a. But using directly this command does not solve the issues relative to the surfaces interface. To solve it a ploy has been used. before to use the $deleteface$ command, the bottom surface of the carved disc has been moved toward the second shim, in order to overlap the two

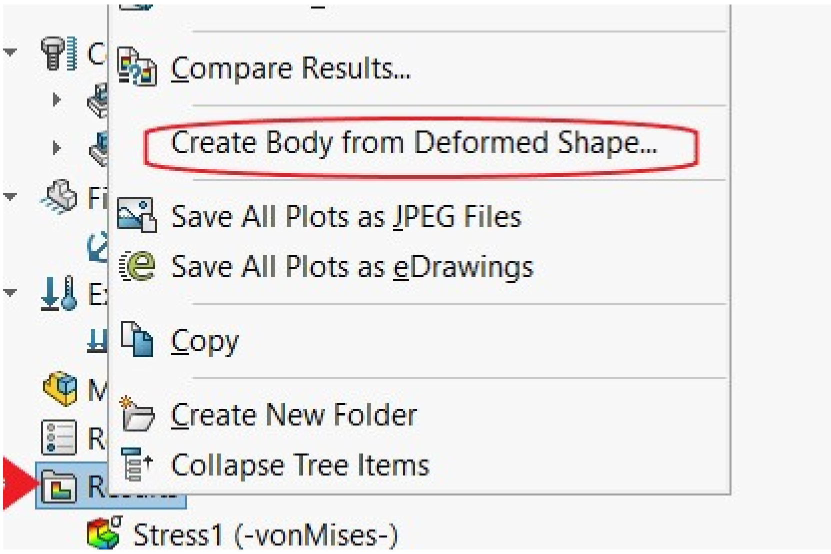

Figure A.1: Create body from deformed shape tool.

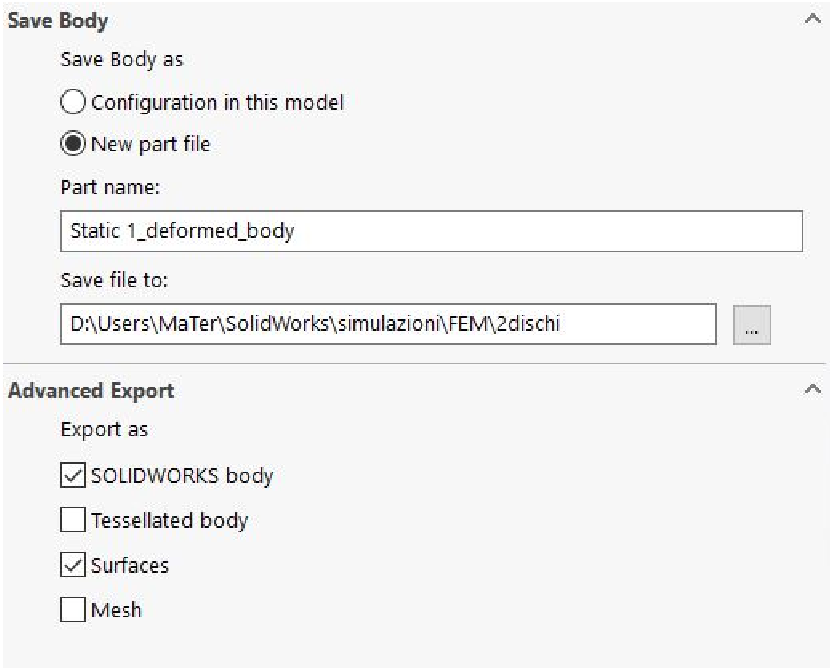

Figure A.2: Create body from deformed shape options.

groups of surfaces representatives of the 2 shims. After that it is possible to transform the volume delimited by the surfaces in solid bodies. The two ones are now overlapping and can be joined by using the command *intersect*. The result of this features sequence is a unique solid body that externally reflects the deformed shape

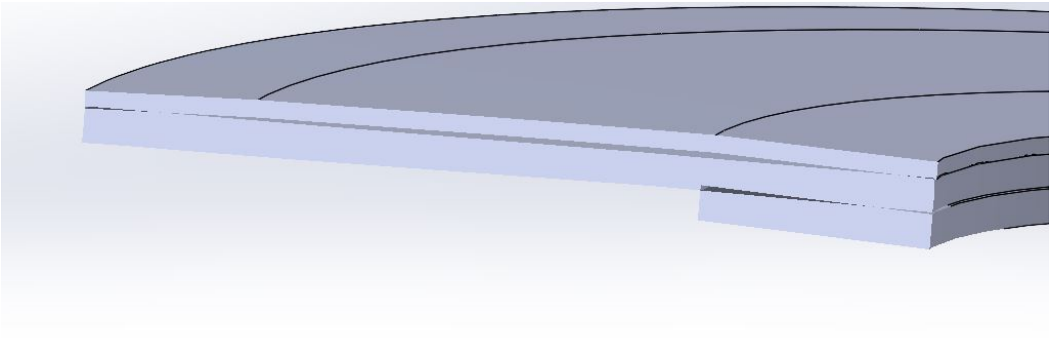

Figure A.3: Shims deformed imported bodies in section view.

coming from the FEM analysis and internally does not present discontinuities, that can affects negatively the CFD simulation. The result of this procedure is shown in figure A.5. Figure A.4b instead shows the list of feature used to reach the objective.

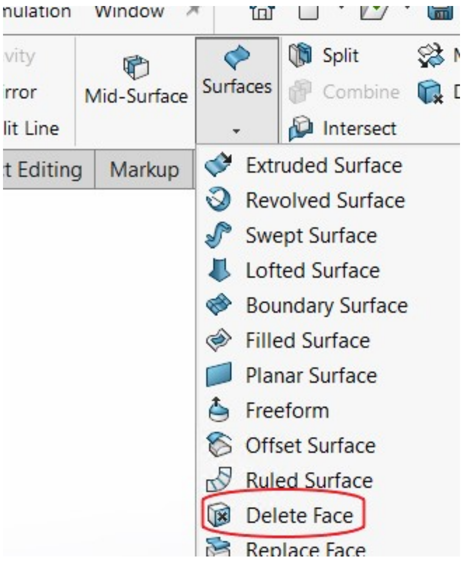

(a) Delete face feature.

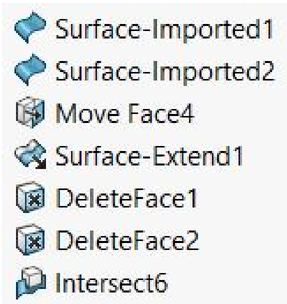

(b) Features list used to create the solid body used in the CFD simulation.

Figure A.4

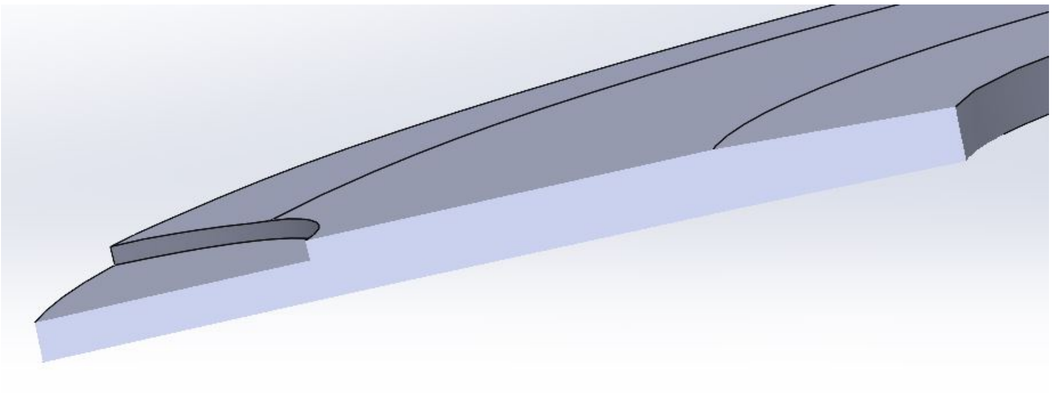

Figure A.5: Final deformed body.

Bibliography

[1] Ermanno Brignolo. "Gli ammrtizzatori oleodinamici: caratteristiche e applicazioni". Mar. 2013. Tesi di laurea, Politecnico di Torino.

[2] John C Dixon. *The shock absorber handbook*. John Wiley, 2007.

[3] G Genta and Lorenzo Morello. *The automotive chassis*. Springer, 2009.

[4] Nicola Nervegna Massimo Rundo. *Passi nell'oleodinamica*. Politeko. Epics, 2020.